GEOTECHNICAL IMPACTS OF AUGUST 2018 FLOODS OF KERALA, INDIA

Event: August 2018

Authors: Thomas Oommen (Leader), Richard Coffman, K. S. Sajinkumar, and C. L. Vishnu

Geotechnical Extreme Events Reconnaissance
Turning Disaster into Knowledge
Sponsored by the National Science Foundation
GEER Association Report NO - 058
Date: 10-17-2018
doi:10.18118/G6ZH3K

Contents

Acknowledgements

The National Science Foundation (NSF) through the Geotechnical Engineering Program under Grant No. CMMI-1266418 supported our visit to Kerala, India in the aftermath of 2018 August Flooding. Any opinions, findings, and conclusions or recommendations expressed in this report are those of the authors and do not necessarily reflect the views of the NSF.

The Geotechnical Extreme Events Reconnaissance (GEER) Association exists due to the vision and support of the NSF Geotechnical Engineering Program Directors: Dr. Richard Fragaszy and the late Dr. Cliff Astill. GEER members also donate their time, talent, and resources to collect perishable data and field observations of geotechnical effects of extreme events. The GEER Association web site, http://www.geerassociation.org, contains additional information. The GEER mission to Kerala, India benefitted greatly from the organizational support provided by GEER Steering Committee Chair, Jonathan Bray.

The reconnaissance team members, included Dr. Thomas Oommen (Michigan Tech), Dr. Rick Coffman (University of Arkansas). Dr. Sajinkumar K.S. (University of Kerala), and Vishnu C.L (University of Kerala). All the team members worked hard to collect perishable data during the reconnaissance trip and contributed to the preparation of this report. The reconnaissance team would also like to acknowledge the contributions of the following individuals or organizations to the success of our mission:

- Dr. R. B. Binoj Kumar (Head of the Department of Geology, University of Kerala)
- Mr. Jeevan Babu, District Collector, Idukki
- State Geologist, Idukki
- Kerala State Department of Mining and Geology
- Information & Public Relations Department for providing video and photographs from the flooding.
- Media personnel
- Kerala Information & Public Relations Department

Cover Photograph – *View of the three open shutters of the Cheruthoni Dam in the background. The Cheruthoni Bridge has been destroyed due to flood waters.* Credit: I&PRD, Government of Kerala.

STATEMENT OF GENERAL LIABILITY LIMITATION – DISCLAIMER

The team who performed this reconnaissance mission is comprised of individual volunteers. The findings and observations presented in this report are based on the conditions of the observed features at the time of the inspection and their experience with other similar structures. This report is not an assessment of condition or safety of the structures observed. No warranty or guarantee regarding the performance or safety of the observed structures is included or intended. Any use of or reliance on this report is at the sole risk of the party using or relying on the report.

Summary

The Southern State of Kerala in India experienced extreme rain in August from the 1st to the 20th, 2018. The state received a cumulative rainfall of 771 mm during that period, which is 140% more than the normal for that time period. The extreme rain event led to flooding and landslide hazards leading to 483 deaths and severe destruction of property. The NSF sponsored GEER team members (Dr. Thomas Oommen, Michigan Tech; Dr. Richard Coffman, University of Arkansas) in coordination with colleagues from University of Kerala (Dr. Sajinkumar K.S. & C.L. Vishnu) conducted a reconnaissance study to gather perishable data. The study was carried out from September 4th to 9th, 2018. The team traveled to three districts that have been affected by the disaster (Alleppey, Idukki, & Ernakulam). The details of the trip and the data collected are summarized in the subsequent chapters. The preliminary finding indicates that the failure of bund in Alleppey further aggravated the flooding and led to the slow recession of flood waters. The flooding in Alleppey has also led to the differential settlement of several buildings. In the district of Idukki, several landslides were identified near recent construction. The alteration in the topography for construction has led to more infiltration and increased groundwater levels during the rain event that have led to these landslides. In addition, soil piping and subsurface drainage channels were also frequently identified at landslide sites in Idukki. This is a preliminary report that the team has produced. A detailed report will be submitted in 3 months.

Chapter 1 - Introduction

Background

Severe floods affected the South Indian state of Kerala from the 8th to the 20th of August 2018. Being a narrow strip of land placed between the Arabian Sea and the Western Ghats and home to 44 rain fed rivers, 34 lakes, and 58 dams (Kerala Geography & History, 2018; Flood Management, 2018), the state of Kerala is highly vulnerable to floods. It is customary for the low lying Kuttanad wetlands to be flooded every year during the monsoons (Kannan, 1979). This calls for a population that should be ready to face water level rises. Still, more than 1 million people had to be displaced and 483 were declared dead during the August 2018 floods (Kerala Floods…, 2018). The heavy rainfall, a cumulative amount of 771 mm from August 1-20 - 140% more than the expected normal (In just 20 days…, 2018), led to numerous landslides and debris flows washing away bridges and roads and cutting off towns and villages besides causing heavy loss of life. The state is yet to completely recover from the damage. Coordinated effort has been put up by the governments and the population to shake-off the material and psychological damage. The Government of India had already declared the floods as a level 3 calamity or 'a calamity of severe nature' (State Faced…, 2018).

The National Science Foundation (NSF) sponsored Geotechnical Extreme Events Reconnaissance (GEER) Association mobilized a team to investigate the potential impact of the heavy rainfall, especially through large scale flooding and landslide activity. The team was led by Dr. Thomas Oommen, Associate Professor, Michigan Technological University and Dr. Richard Coffman, Associate Professor, University of Arkansas. The logistics for the trip was planned by Dr. Sajin Kumar K.S, Assistant Professor, Department of Geology, University of Kerala. The main objective of the field visit was to collect perishable data associated with such a disaster. Collecting the perishable data immediately after the disaster can be extremely valuable to validate future detailed field or remote sensing analysis (Sahoo et al. 2007; Oommen et al. 2013; Bouali et al. 2016). The team visited the flood and landslide affected areas in Kerala from 3 to 9 September 2018.

The recent flood in Kerala provided an opportunity to investigate the geotechnical impacts of flooding on infrastructure. The team focused on understanding how the flood and landslides affected roads, bridges, and dams. The team also documented the impact of these events on foundation, coastal structures, and slopes and embankments. Collaborations with local scientists and engineers, such as those from the Geological Survey of India, and State Department of Mining and Geology officials were beneficial for the on-field investigation.

The team visited three districts in Kerala: Alappuzha, Ernakulam, and Idukki. The GEER team approached Alappuzha and Idukki as a representative location for studying flood and landslide hazards, respectively. In Alappuzha district, importance was given to the Kuttanad region. Kuttanad is below Mean Sea Level (MSL) region known for its wetlands and backwaters. It is in fact the lowest area in India with elevations as low as 2.5 meters below sea level (Simon & Jacob, 2013). Known as the Venice of the East, Kuttanad is the 'rice bowl' of Kerala, with its far spreading paddy lands. The flood in this area was particularly detrimental as large areas of crop suffered damage. The Pamba, Achankovil, Meenachil and Manimala rivers flow into this region. Kuttanad was heavily flooded and the flood water had not receded even during the GEER team visit, which was held on 4th September. Certain buildings were tilted and developed cracks, indicating land subsidence as a result of heavy floods. Soil strength tests were carried out in these sites. Flood level was demarcated and coordinates were recorded using Differential Global Positioning System (DGPS). The team stayed in Kuttanad for the 4th and 5th September.

From 6th to 9th, the team visited the landslide prone areas in the Idukki district. The Idukki district is in the highland region of the state and is famous for many hill stations like Munnar and Vagamon. Idukki is the most landslide susceptible district in Kerala. This monsoon season alone, Idukki saw 278 landslides, which claimed 46 lives and destroyed more than 100 acres of property. Even during the visit of the GEER team, many roads were rendered unapproachable due to landslide debris and structural collapse. The peculiar geology of Idukki which comprises of steep slopes and a loose layer of soil that rests on hard rock without adhesion is a major factor for recurring landslides. Many noteworthy

landslides were observed and studied in various places, such as Kattappana, Nedumkandam, Mavadi, and Munnar. Heavy structural damages were incurred by many buildings in these regions. These structures were also studied and evidences were collected. The Kulamavu and Idukki dams were also visited and data were collected.

Topography, Geology, and Climate of Kerala

Kerala is a state located in the South Western part of peninsular India. The state is bordered by Tamil Nadu in the east, Karnataka in the north and the Arabian Sea in the west. The state lies between 8.3º and 12.8º north latitudes and 74.86667º and 77.86667º east longitudes (Narendra Prasad, 1998). The topography of Kerala can be divided into three parts: the highlands, midlands and the lowlands (Chattopadhyay and Franke, 2006). The highlands of the Western Ghats comprises almost half the area of the state and houses large peaks like the Anaimudi with a height of 2694 m. The highlands are predominantly forest covered though they are home to tea, coffee and cardamom plantations. The midlands occupy roughly 40% of the state and have an undulating topography of hills and valleys. Most of the midlands are home to urban settlements and agriculture. The western coastal plains form the lowlands. This low lying area comprises lagoons, river deltas, backwaters, and beaches. Figure 1.1 shows the study area in detail.

Kerala has a tropical maritime climate. The state receives abundant rainfall from two monsoons: the south west monsoons during June–September and the north-east monsoons during October-December. A mean annual rainfall of 2693 mm occurs over 120-140 rainy days. The south-west monsoon provides for 60% of this rainfall. The mean annual temperature is a steady 25.4ºC to 31ºC in the midlands while the highlands have an average of 15ºC. The state has a humid climate with the mean relative humidity between 85% and 95% during the monsoons and around 70% during the summer.

Kerala constitutes four major geologic formations: crystalline rocks of Archean age, sedimentary rocks of the Tertiary age, laterite capping on crystalline and sedimentary rocks and Recent sediments (Chattopadyay and Fanke, 2006). Being part of the South Indian Precambrian terrain, The State consists of granulites, gneisses, granites, and greenstones and they are mainly seen in

the midland and highland. The Tertiary sedimentary are confined to the coastal plains. The Tertiary and crystalline formations in the midlands are found as lateritized units that act as good aquifers. Alluvial deposits of Recent origin are also found along the coastal regions.

The 2018 Kerala Floods

The major events of the flood unfolded in a period from the 8th to 20th August, 2018. On 8th, Kerala received a rainfall of 310 mm in 24 hours. Shutters of the Neyyar Dam in Thiruvananthapuram district was raised by 5 inches. The Chalakkudy River in the Thrissur district overflowed. By then, the Upper Kuttanad region was already inundated. Landslides of noticeable magnitude started to be reported and hundreds of families were left isolated.

On 9th, one gate of the Idukki dam, which is the largest arch dam in Asia, was opened. The last time this gate was open was 26 years ago. Shutters of the Idamalayar dam and other 22 dams across the state were opened. More landslide events were reported along the Malappuram, Idukki, Wayanad, Kannur, Kozhikode and Palakkad districts. By then, almost 8000 people were evacuated to relief camps.

By the 10th of August, half the districts of Kerala were declared flood-hit. More than 10,000 people were evacuated. Army personnel were deployed for rescue and relief missions in Idukki district, which was heavily hit by landslides. The Cochin airport, the largest in the state, was shut down due to flooding of the runway.

By the 11th of August, around 60,000 people were evacuated to relief camps. The Indian Meteorological Department (IMD) issued a red alert on 8 districts. The water level in Idukki dam crossed 2400 feet, close to its full capacity of 2404 feet. The situation in Kuttanad region was getting worse due to increased rainfall.

On 12th August, a low-pressure formation was observed over the Odisha coast and heavy rainfalls were predicted over Kerala for the next 2 days. An estimated 20,000 houses were damaged by this time and over 30 people were declared dead.

By the 13th August, 302 relief and rescue camps had to be open across the state. Frequent landslide reports were emanating from the highland regions of the state.

On August 14, all the gates of the Idukki dam had to be opened. The Pampa River experienced the worst floods in half a century. The high-range town Munnar was completely isolated due to roads being damaged by landslides.

On August 15, for the first time in history, the gates of 35 dams in the state remained open simultaneously. 8 persons were declared dead as a house collapsed in Malappuram.

By the 16th of August a total of 105 people were officially declared dead due to floods and landslides. The Idukki district received 84% increased rainfall. The water levels at the Idukki and Mullaperiyar dams reached dangerously close to their full capacities. Eighty seven (87) locations in the state reported landslide events as thousands were left isolated. The upper Kuttanad region was completely flooded. The transport network in the state was disrupted in many parts and the Southern Railways and Kochi Metro services were suspended. The water supply in Ernakulam district was completely disrupted. More army and navy units were deployed for rescue and relief operations.

By the 17th of August, 150,000 homes were abandoned in the Kuttanad region. Over 300,000 people were relocated to rescue and relief camps by now. The Kerala State Electricity Board switched off the power supplies of over 4000 transformers across the

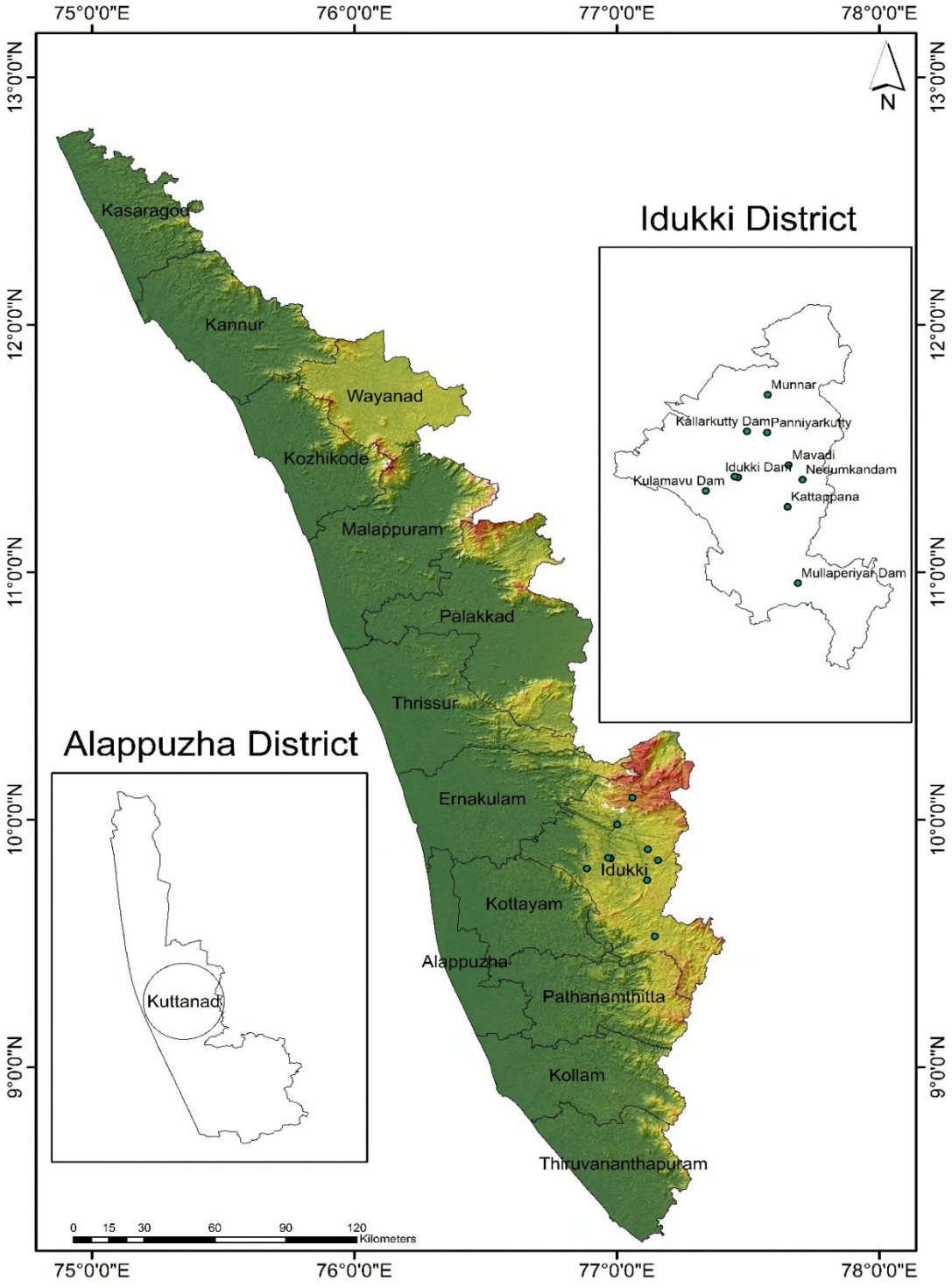

Figure 1.1: *Kerala State. The insets show the Idukki and Alappuzha Districts – locations of the GEER team field visit*

state. The cities of Thiruvalla, Chalakkudy, Chengannur, and Kalady were isolated and flooded. The fishermen from Thiruvananthapuram joined the rescue operations along with the military forces due to the unprecedented nature of the fast spreading disaster.

On the 18th of August, the floods hit peak values. The death toll rose to 195. Alappuzha and Ernakulam districts were almost submerged. Many highways were blocked, stranding people and obstructing rescue operations. The cities Chalakkudy, Aluva, Chengannur, Paravur, Mala, Kalady and Thiruvalla, Ranni, Panthalam, Kozhanchery were critically inundated.

On the 19th of August, the rainfall decreased and the floods started to recede. Rescue operations were in full swing and affected people were being quickly relocated to relief camps. Ninety percent (90%) of the Kuttanad residents were evacuated. People were still stranded in many cities, including Chengannur and Paravur. Over 700,000 people were in relief camps by now and 220 people were declared dead.

On 20th August, the IMD officially declared that rainfall intensity will remain below alarming levels in the coming days. Rescue operations were nearing completion. Over 1 million people were in relief camps. 11,000 houses and 46,000 hectares of crop were officially declared destroyed. 252 people were declared dead.

The inventory of damages later prepared by the government showed an even meek picture. A total of 483 people were declared dead and another 14 went missing. It was the worst flooding in Kerala in nearly a century. According to the Kerala government, one-sixth of the total population of Kerala had been directly affected by the floods and related incidents. The Indian government had declared it a Level 3 Calamity, or ‘calamity of a severe nature’. It is the worst flood in Kerala after the ‘Great Flood of 99’ that happened in 1924.

A combination of various factors is understood to be the root cause of the flood. The above normal rainfall during the monsoon season is considered to be the most important factor among them. The 2018 monsoon saw extreme rainfall events all through the state. The summer monsoon rainfall in

Kerala from May to August this year was 2,290 mm, which was 53% above normal range. The average rainfall during the summer monsoon period (June-September) is about 1,619 mm. This makes 2018 Kerala's third wettest year in the last 118 years (1901-2018); 1924 and 1961 were the wettest years with about 3,600 mm of annual rainfall.

Over 90% of the reservoir storage was reached even before the onset of the main flooding event. This caused large discharge of water from the reservoirs during the period of the main flood. The heavy downpour during these days, especially in the catchment of these reservoirs made this matter worse. Moreover, the flooding event coincided with the period of high tide. Thus, the excess discharge from the rivers could not be drained effectively into the ocean, thereby causing an increased water level rise in the inland. This scenario particularly affected the low lying Kuttanad and Kole wetlands. Figure 1.2 shows a flood inundation map prepared from the satellite Sentinel 1. It marks the flood in the central part of Kerala, especially the Kuttanad and Kole wetlands.

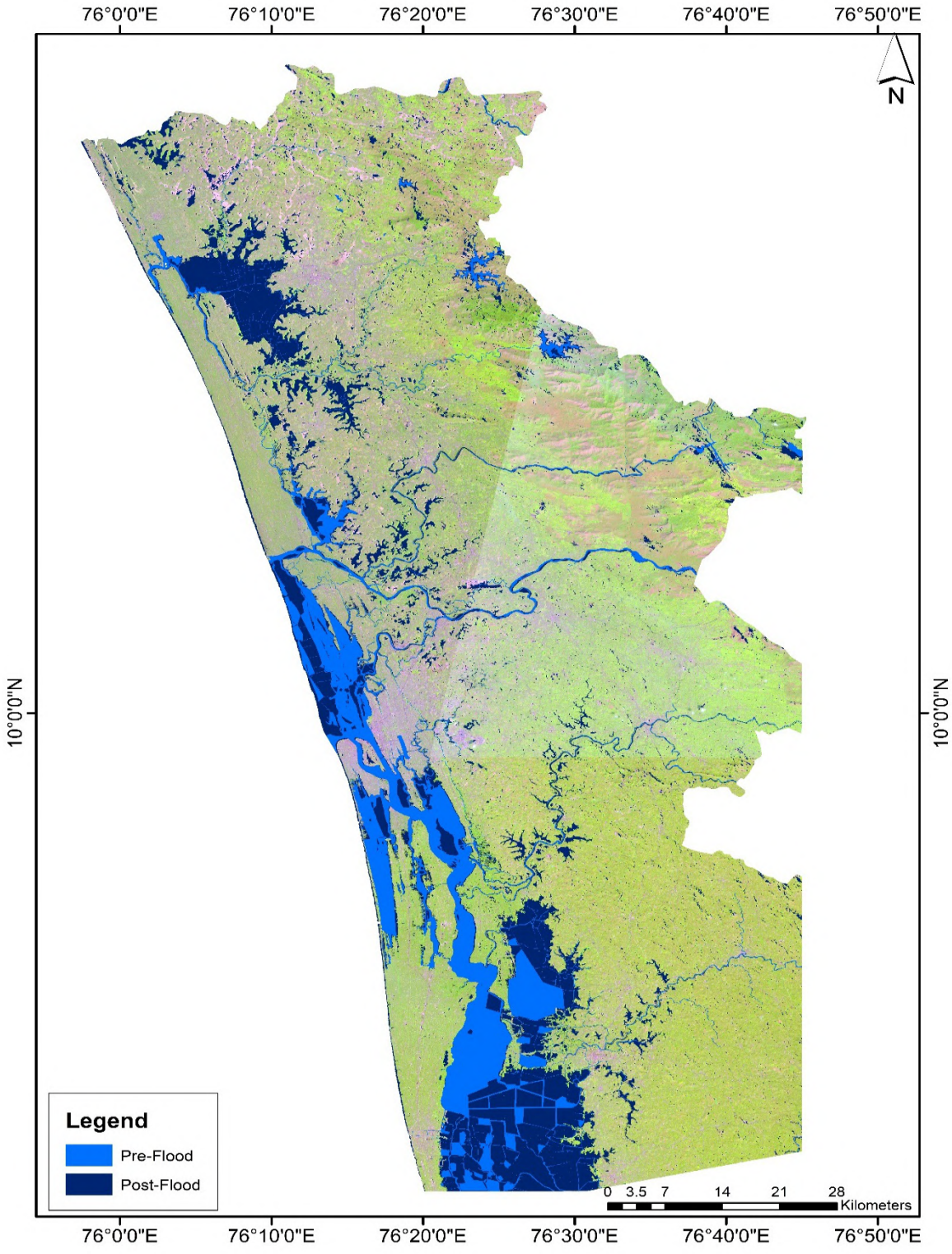

Figure 1.2: *Central Kerala before and after flood*

Chapter 2 - Landslides and Debris Flows

Introduction

The Western Ghats, the bold westerly escarpment of India (Radhakrishna 2001), bears the testimony of frequent landslides, especially during the monsoon season, and it causes widespread damage to life and property (Sajinkumar et al. 2011). About 8% (1,400 km^2) of area in the Western Ghats of Kerala is classified as a critical zone for mass movements (Thampi et al. 1995; Sajinkumar and Oommen 2018) (Fig 2.1). This region is characterized by rugged hills with steep long side slopes on which rests the loose unconsolidated soil and earth material (Thampi et al. 1995). Oversaturation of slopes fractured by tectonic forces, affected by weathering processes and compounded by anthropogenic interface leads to frequent slope failure in this highly rugged mountain system (Thampi et al. 1995; Sajinkumar et al. 2014a). This mountain range has been affected by landslides of differing form, scale and dimension ranging from rock fall, rock slide, debris slide, debris fall, debris flow, debris avalanche, and slump and creep to subsidence (Anbazhagan and Sajinkumar 2011; Sajinkumar et al. 2014a, b; Sajinkumar and Anbazahagan 2015; Sajinkumar and Rani 2015). Most of the landslides occur during the monsoon season and hence, rainfall is considered as the dominant triggering mechanism (Sajinkumar 2005). Moreover Sajinkumar et al. (2011) noted that hills capped by thin veneer of soil and steep slope results in landslide.

Landslides in Kerala, India, have been shown to be preceded not only by critical rainfall over a short period but also a much longer period of elevated pore pressure (Weidner et al. 2018; Oommen et al. 2018). Such rainfall triggered landslides are difficult to monitor due to a lack of adequate data on the locations of failures and precipitation. Hence, analyzing and correlating rainfall threshold with Factor of Safety (FS) for landslides can be valuable to develop an early warning system, especially in tropical regions proverbially prone to landslides. The development of a composite model can assist in devising a simple, cost-effective, and comprehensible early-warning system for shallow landslides (Shruti Naidu et al. 2018). In such models, it is critical to understand the rainfall threshold and the susceptibility of the slope to landslide hazard (Bíl et al. 2015; Montrasio et al. 2007; Smith et al. 2015). Such an early warning system can be developed

on a site-specific basis and may be generalized for regions that have similar climatological and topographical conditions. An early-warning system is an essential requirement for landslide prone localities as it could reduce the losses and casualties that accompany natural hazards.

Geological history suggests that there is no representation of Phanerozoic above the Precambrian crystallines except a thin veneer of recent sediments (Soman, 2002; GSI, 2005). The prevalence of tropical climate enhanced the chemical weathering (Sajinkumar et al, 2011, Sajinkumar et al, 2015) and facilitated the formation of a thick column of soil over the Precambrian crystallines (Sundarajan and Sajinkumar, 2012) wherever the topography permitted, such as the Munnar Plateau and Wayanad Plateau. This unconformity, existing between the Precambrian crystallines and the overlying recent sediments, forms the slip plane for the landslides in Kerala. The typical landslide dynamic type occurring in Kerala is debris flow restricted to monsoon period (Sajinkumar and Anbazhagan, 2015). Hence, in most cases, the area now affected by landslides will be free from landslides in the future as the entire debris will be washed away by the landslides.

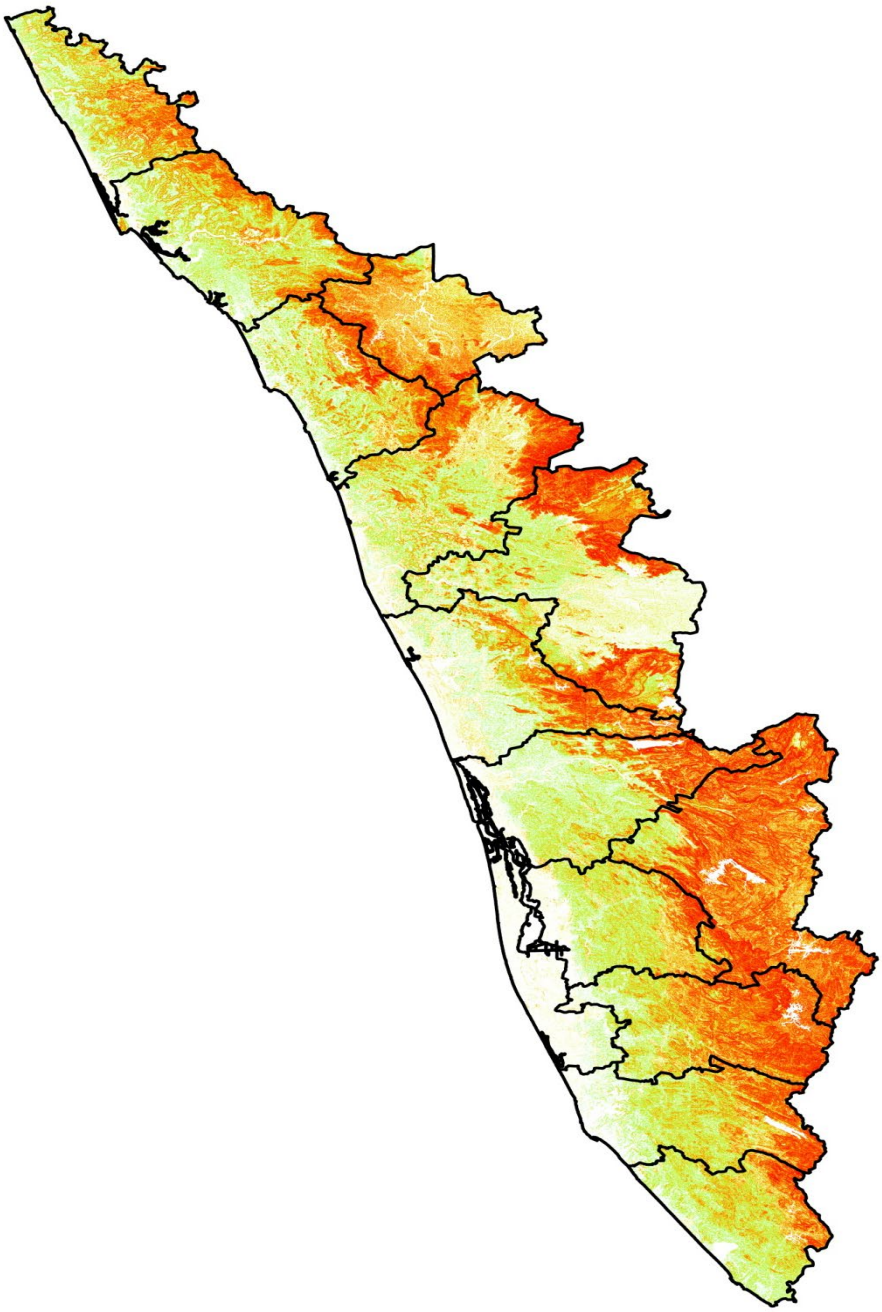

Figure 2.1: *Landslide susceptibility map of Kerala (Source: Sajinkumar and Oommen, 2018)*

Background

Being in tropical climate, the state of Kerala, India experiences monsoon. It is characterized by two spells of monsoon: Southwest monsoon (SWM) during June-September and Northeast Monsoon (NEM) during October-December. During 2018 SWM rainfall events, between June 1 and August 29, the amount of rainfall was 36-percent more than the normal rainfall for that period (IMD, 2018). Sporadic events of intense rainfall (e.g. 177.5 mm on August 17, 2018, at Idukki) in the Western Ghats triggered several landslides and inundated parts of the Pathanamthitta, Alappuzha, Kottayam, Idukki, Ernakulam, Thrissur and Wayanad districts. Moreover, the floodwaters that resulted from the dam release disrupted the life of hundreds of thousands of citizens and warranted the need to open safe shelters to the affected populations. This extreme event resulted in 445 deaths, uprooting several trees and poles, partial or complete movement or water-logging of homes, shops, roads, and other civil infrastructure, and caused heavy siltation over the affected land.

Summary of Sites and Main Mechanisms of Failure

Idukki and Wayanad are the main landslide affected areas. Due to the limited time, the team visited only Idukki district. Geologically, Idukki district forms a part of the Madurai granulite block (MGB) of the southern granulite terrain (SGT). The lithology of the area is characterized by hornblende gneiss (including hornblende-biotite and quartz-mica gneiss) and pink granite gneiss (Munnar granite). Hornblende gneiss is formed by the retrogressive metamorphism of charnockite due to the emplacement of granite. With charnockite, it shows gradational, irregular and sharp contacts (Rajan et al., 1984). Pink granite gneiss or Munnar granite pluton, with minor phases of syenite and carbonatite emplaced within Precambrian gneisses, is spatially related to the intersection zone of the NE-SW Attur lineament and NW-SE trending Idamalayar lineament (Santosh et al., 1987). This alkali granite has been dated at 740±30 Ma (Odom,1982).

Geomorphologically, the district shows diverse features from the towering Anaimudi hills (2695 m above msl) to the midlands in Thodupuzha. The most conspicuous feature is the Munnar plateau, which is the largest and highest plateau in Kerala. Though named a plateau, this area is dotted by denudation as well as isolated structural hills, and has alternate valleys and ridges. The

slope varies but is generally steep (>30°). The soils are mainly lateritic with typical reddish color and with high clay content.

The hills of Idukki are home to different cash crops. Tea gardens, rubber plantation, forest, and settlement with mixed cultivation are the major land use of this area. Eucalyptus and acacia, planted under the government's social forestry scheme, occupy the major part of the forest, whereas the upslope portions are occupied by degraded forests and shola grasslands (meadows/prairie).

The landslides occurred in Idukki can be broadly divided into the following categories:

1. Shallow-seated landslides: Most of the landslides that occur in Kerala are shallow in nature as the overburden occupying the highly dissected hilly topography in Idukki district ranges from 0 to 4 m in thickness. This soil belongs to the recent category and rest in the Precambrian rocks and hence, has less adhesion between these two lithounits. In most cases, this soil gets saturated by a 2 to 5 days spell of rain. As landslide occurs, the soil gets washed away through the soil-rock interface plane.
2. Deep-seated landslides: Deep-seated landslides are confined to plateau region where the thickness of soil exceeds 5 m (at places reach 20 m). The prevalence of tropical climate enhanced the chemical weathering (Sajinkumar et al, 2011, Sajinkumar et al, 2015a) and facilitated the formation of a thick column of soil over the Precambrian crystallines (Sundarajan and Sajinkumar, 2012) wherever topography permitted, such as in the plateau region. Therefore, the landslides occurring in such geomorphic conditions will have more devastation and bigger dimension.
3. Piping: The overburden material seen in the hilly part of Kerala are unconsolidated and consists of varying amounts of clay, sand, and gravels. The subsurface flow usually removes the clay content and facilitates the formation of cavities of differing dimensions and gets interconnected in due course of time. During rainy season, these interconnected cavities act as conduits for water discharge and favor the internal soil erosion. The phenomenon of development of these conduits is called piping. Such conduits facilitates

the occurrence of landslides (Sarkar 2011). The piping phenomena was well documented by Pierson (1983); McDonnell (1990) and Uchida et al. (2001).

4. Partially failed landslides: Partially failed landslide or 'aborted' landslides have occurred in different places, especially in areas with gentle slope (15-22°), which are generally considered free from landslides. The manifestation of such landslides is development of concentric curvilinear cracks running for several tens of meters and sometimes, hundreds of meters. The curvilinear crack matches with the shape of the crown of a landslide. These cracks at place have imparted a step-like topography to the area wherein each step differs from the adjacent steps by an elevation difference of about 3–5 m.

Select Landslide Cases

1. Nirmala City landslides (9.7925061^{0}N; 77.0680952^{0}E): Several landslides have occurred in Nirmala City near Kattappana that resulted in destruction of 10 houses. Most of the landslides fall in two categories: (a) Partially failed landslide and (b) Cut-slope failure. The partially failed landslide was confined to a gully of a lower order seasonal stream. Such features are called topographic hollows. The constructional activities along such natural paths blocked the excess water from discharging. Moreover, the hill consists of a shallow abandoned dug well that was meant for domestic purposes. All these facilitated the percolation of rain water and subsequent increase in pore-water pressure. About 10 houses, wholly or partially, was destroyed in this event. A metalled road was displaced for about 1 m (Fig 2.2a).

The cut-slope failure occurred in a slope modified for constructing a house. Almost 6 m thick overburden was excavated for the construction of a house. This facilitated the water percolation and caused the landslide. A further 3 m thick soil, downhill of this excavation, was removed by this landslide (Fig 2.2b). This landslide has made the area/house unoccupied. Further possibility of landslide, with a head-ward retreat, is possible in an anomalous rainfall such as this.

2. Mavadi landslide (9.8747275°N; 77.1194017°E): A noteworthy landslide that occurred at Mavadi was the collapse of a building wherein a single-storey building was completely undergone subsidence (Fig 2.3). At a glance it looked like a subsidence. But a closer observation

showed that it was a partially failed landslide. The upper part of the landslide has failed whereas the rest of the part was partially failed, manifested as land disturbance. The land disturbance varies from 0.5 m to 2 m. This area has a comparatively gentler slope (15-22°) and hence, is free from landslides during early periods. The rainfall should be the only factor that caused the landslide. The area is expected to receive more rainfall during the North East Monsoon. Hence, such partially failed landslides are the best avenue for further collapse.

3. ***Munnar College landslide (10.0822468°N; 77.0734293°E):*** The landslide happened in the vicinity of the Government College at Munnar, in Idukki. The Munnar Government College Landslide crossed the Munnar-Kumily Highway (also referred to as the Kochi-Madurai-Tondi Point Road). Munnar has the distinction of being in a plateau region at an elevation of ~1,600 m and the thickness of soil usually exceeds 5 m making the landslides deep-seated. In the past, this area had witnessed a landslide on 25th July 2005 (Fig 2.4a). Since this was a holiday for the college, no casualties occurred. This landslide was confined to a cut-slope, excavated for construction of the college building, without considering the slope characteristics or without providing any adequate protective measures. This landslide was studied in detail and was termed as a 'head-ward retreating landslide' (Sajinkumar et al. 2017), expecting it to fail in heavy rainfall. However, the college authorities extended the campus within the landslide scarp, foregoing the warning from previous studies. The same location experienced a major landslide during the recent rain events destroying the college buildings (Fig 2.4b,c). The landslide has uprooted all the structures in its path.

   Dynamic cone penetration tests were performed and electromagnetic spectrum (350-2500nm) were collected at the Munnar Government College Landslide site. The data were collected within a small portion of the slide next to the partially collapsed building. The results from dynamic cone penetration soundings are reported in Figure 2.5 and the spectrum are presented in Figure 2.6. The path that was followed during data collection is presented in Figure 2.7. A crust was observed over the mass wasted soil within the landslide mass. This crust enabled the GEER team to collect data on top of the mass wasted soil, however, caution was taken because the soil underneath the crust was classified as being very soft. One of the Indian counterparts

punched through the crust while walking on the crust. The Indian counterpart had to be assisted to remove the suction that developed between his foot and the underlying soil. The data were collected within a small portion of the slide next to the partially collapsed building.

3. ***Vellathooval landslide (10.0088136°N; 77.0257626°E):*** The landslide at Vellathooval is a classic example of piping (Fig 2.8a). Small conduits of varying dimensions (10-30 cm) are quite obvious in this area (Fig 2.8b). These subsurface conduits carry water and the dimension of the conduits changes with change in the velocity and discharge. The civil structures resting above such conduits will be under threat.

Figure 2.2: (a) Displaced road due to partially failed landslide 9.7968615^0 77.0675334^0 (b) Cut-slope failure at Nirmala City 9.7925061^0 77.0680952^0. Note the modified slope behind the house.

Piping has initiated the landslide and has developed into typical debris flow with approximately 20 m (width), 500 m (length) and 2 m (thick). All the debris was debouched into an adjacent river. This landslide has resulted in 5 deaths and destruction to 5 buildings. Three bodies are yet to be recovered.

Figure 2.3: Collapse and submergence of one storey near Mavadi 9.8747275°N; 77.1194017°E.

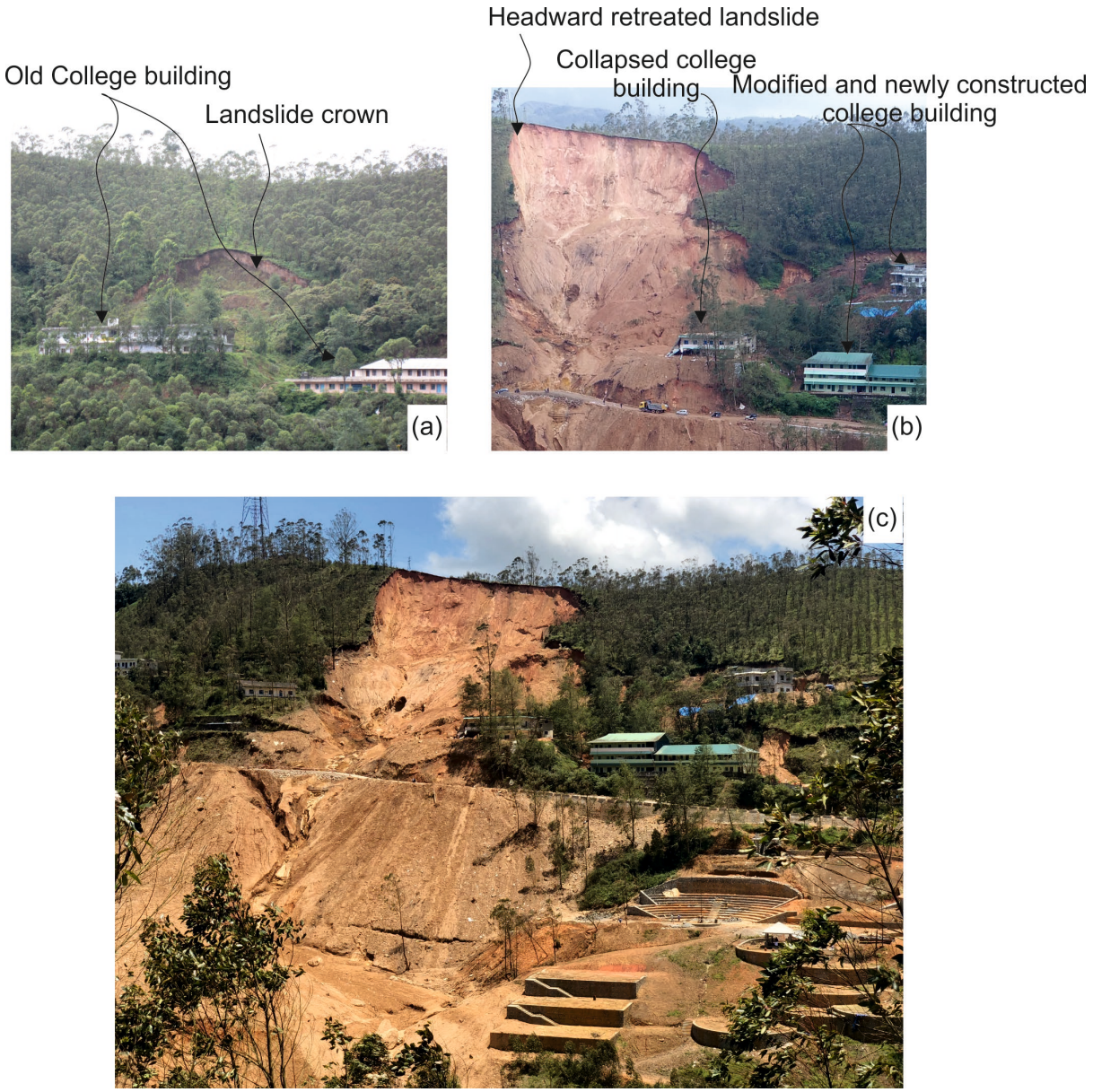

Figure 2.4 (a) Landslide scar of 2004 in the vicinity of Government College Munnar. Note the sagging of the crest line. (b) 2018 landslide uprooting the College building (c) Enlarged view of (b) *10.0822468°N; 77.0734293°E*

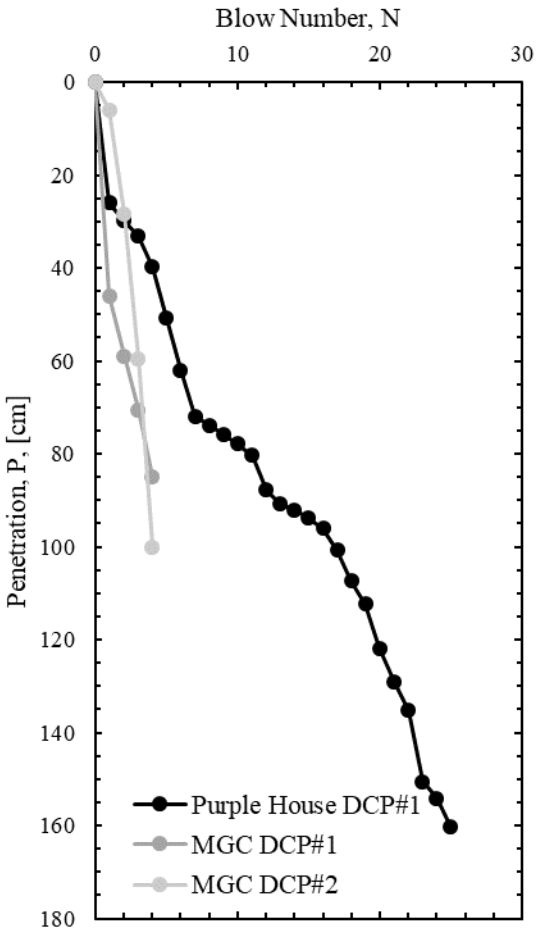

Figure 2.5: *Dynamic cone penetration soundings at the Munar Government College site. Weakest sounding from Alleppey Purple House is shown for comparison.*

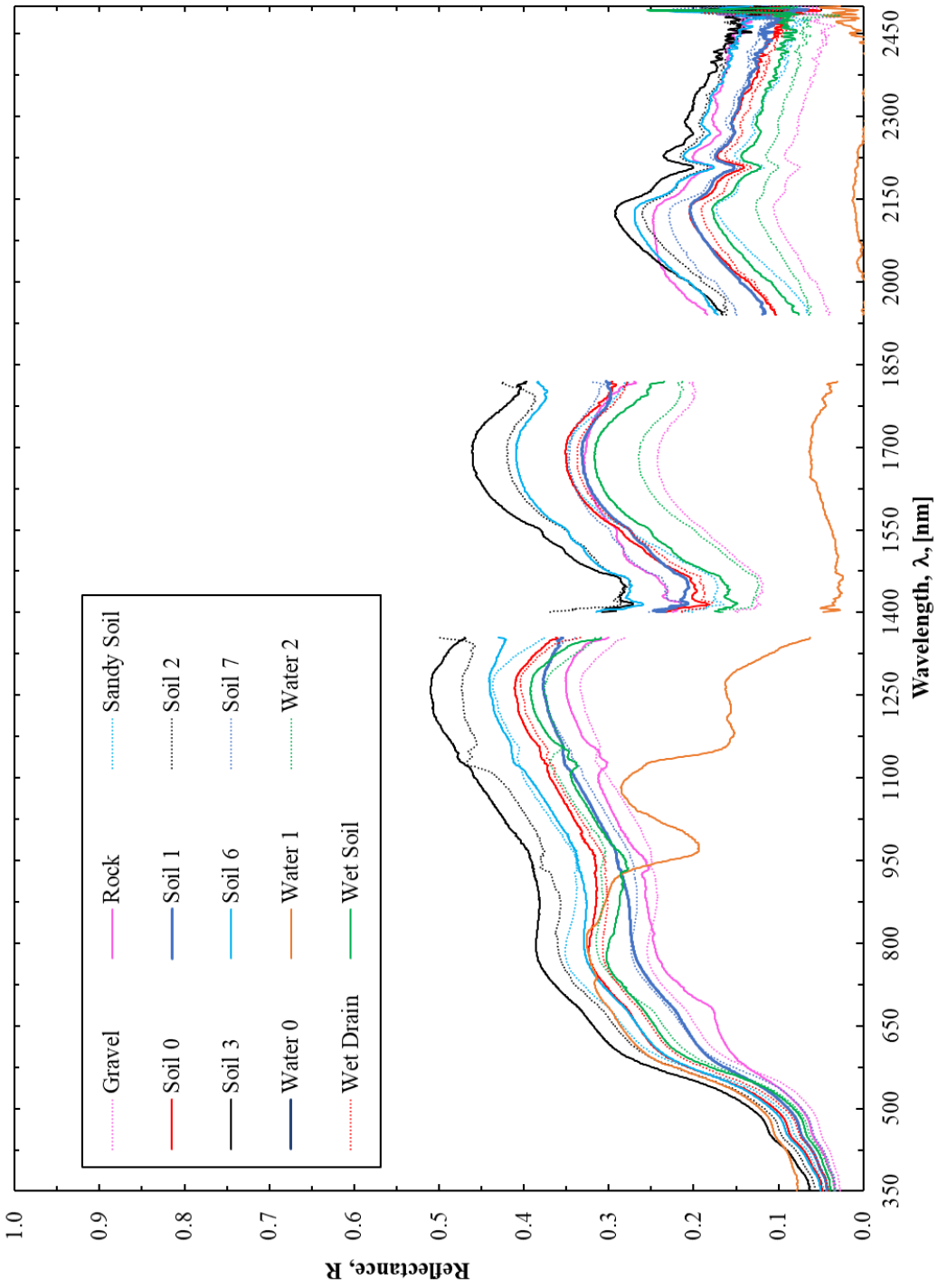

Figure 2.6: *Electromagnetic spectrum collected at the Munar Government College Landslide site. Approximate positions of data collection presented in Figure 2.7.*

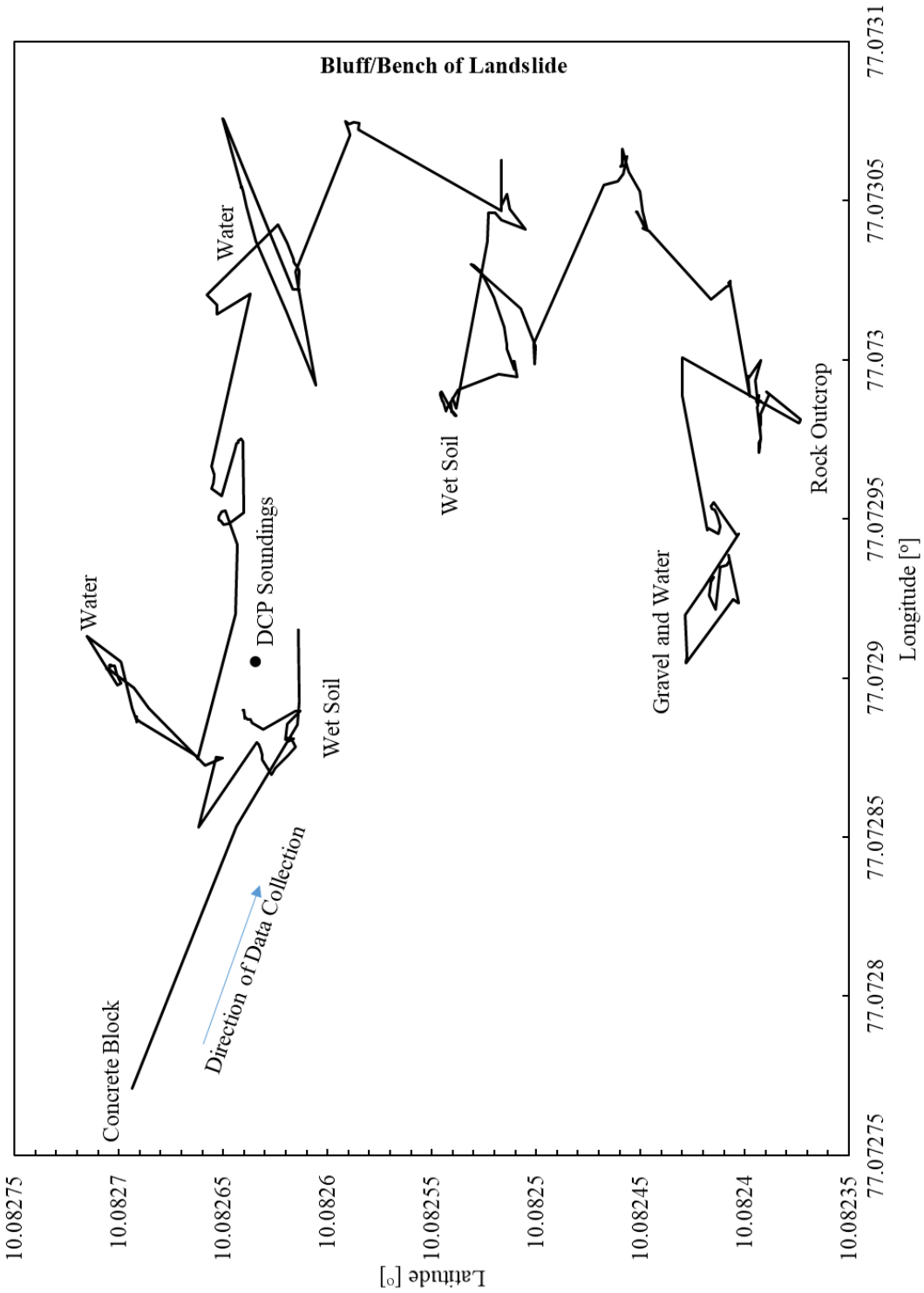

Figure 2.7: *Data collection path for collection of the electromagnetic spectrum and DCP data.*

Figure 2.8 (a) Landslide at Vellathooval (b) Surface manifestation of a conduit in piping phenomena 10.0088136°N; 77.0257626°E

4. Kattappana Landslide (9.76461°N; 77.1095°E):

The Kattappana Landslide was encountered while in transit from the Idukki Landslide (Latitude=9.79655º, Longitude=77.0685º) to the collapsed house in Mavady (Latitude=9.8747º, Longitude=77.1194º). Time was limited on this site because the GEER team and Indian-counterparts were expected to meet a news crew at the location of the collapsed house prior to sunset. The team was on site at this location for approximately 10 minutes from 4:40-4:50pm on the afternoon of September 6, 2018 (Figure 2.9). While onsite Dr. Coffman took several photographs from different vantage points. These photographs were sued to develop a three-dimensional reconstruction of the landslide (Figure 2.10). It would have been nice to spend more time at this landslide because the landslide 1) occurred at a location of terracing, 2) appears to be the result of undercutting of the toe of the landslide and 3) failed along a predetermined failure plane that starts at the soil/rock interface that is shown in the photographs in Figure 2.9. As documented in a Twitter post shown in Figure 2.11 (ANI, 2018), the Kattappana Landslide blocked the Thodupuzha-Puliyamanmala roadway (also referred to as Highway 33 or National Highway 185) preventing traffic from Kumily to Idukki.

Figure 2.9: *Photographs of the Kattappana Landslide located at (notice Dr. Coffman within the slide extents preparing to take photographs, Latitude=9.79655º, Longitude=77.0685º).*

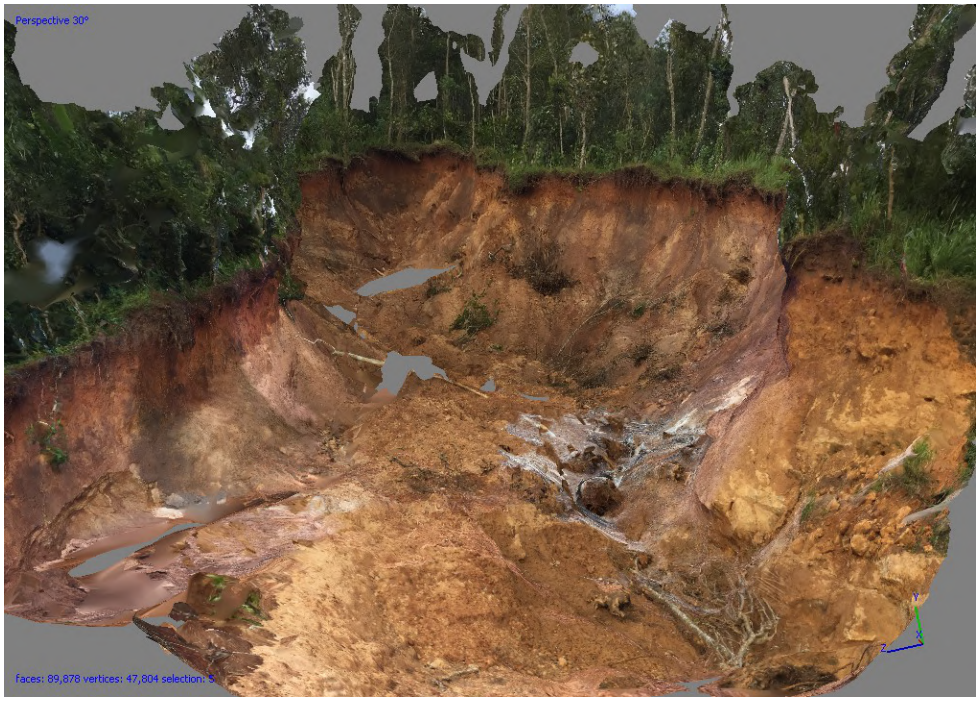

(a)

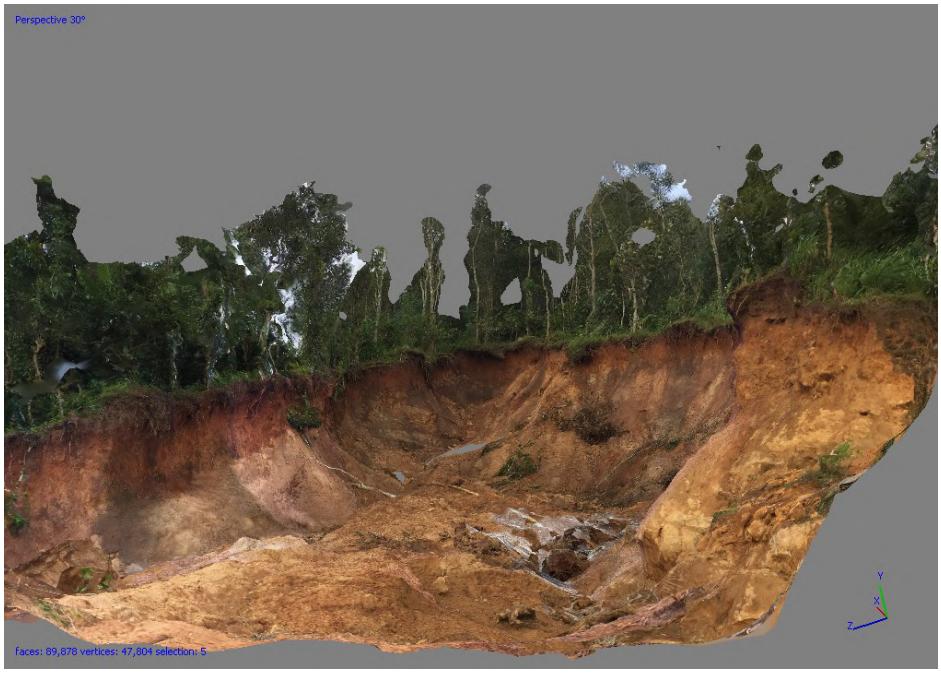

(a)

Figure 2.10: *Three-dimensional reconstruction of Kattappana Landslide by means of Photoscan. (a) left side right side isometric projection, (b) right side isometric projection (Latitude=9.79655°, Longitude=77.0685°).*

Figure 2.11: *Roadway clearing operations at the Kattappana Landslide. The horizontal rebar in the bottom right photograph are also present in many of the photographs taken by the GEER team. Source: Twitter.*

5. Mapping of landslide and structural damage in Idukki: On the afternoon of September 6, 2018, the GEER team and Indian counterparts traveled to landslides located in the Idukki district. The most prominent landslide was mapped by means of global positioning measurements (Figures 2.12 and 2.13) and documented by means of photographs (Figure 2.14). Like with the structural reconstruction of the purple house that is mentioned in the Alleppey section, one of the houses

located within the large landslide was also reconstructed using PhotoScan (Figures 2.15, 2.16, 2.17, & 2.18). This house was selected because of 1) the extensive damage to the structure and 2) for the possibility of doing forensic damage investigations by means of the cracking pattern. As shown in Figure 2.14, it appears that the structure was built in multiple stages and most of the damage occurred at the connection between the original structure and the addition to the original structure. The addition/original structure damage pattern did not appear to start or progress from a location of head scarp movement or block-wedge movement. Therefore, it is believed that the damage location was a function of different modulus and rigidity values for the different portions of the structure.

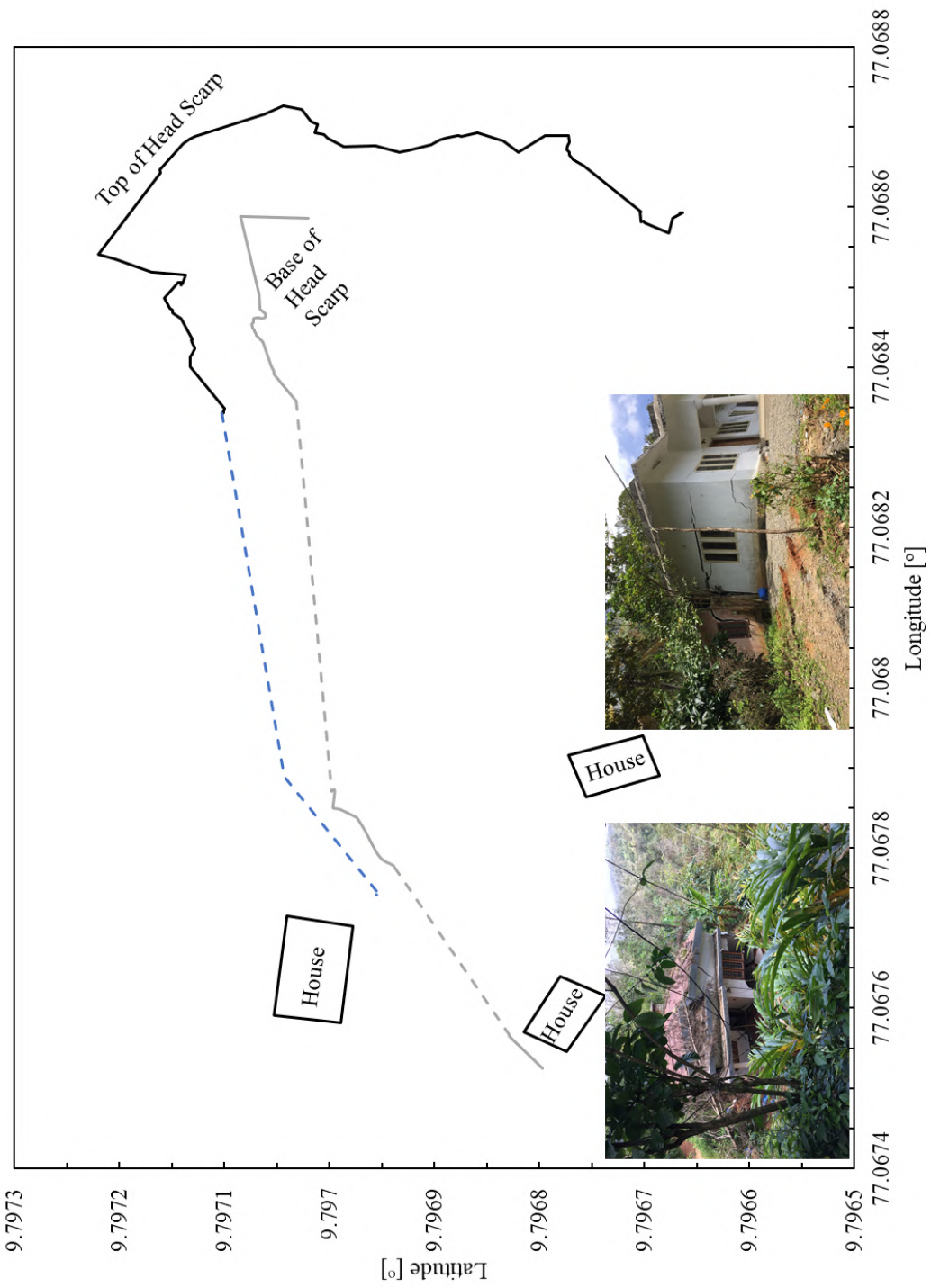

Figure 2.12: *GPS coordinates (latitude and longitude) of the top and toe of the headscarp of the largest Idukki landslide that was investigated. Locations and photographs of houses within the landslide included for completeness. Dashed lines represent interpolated landslide extents.*

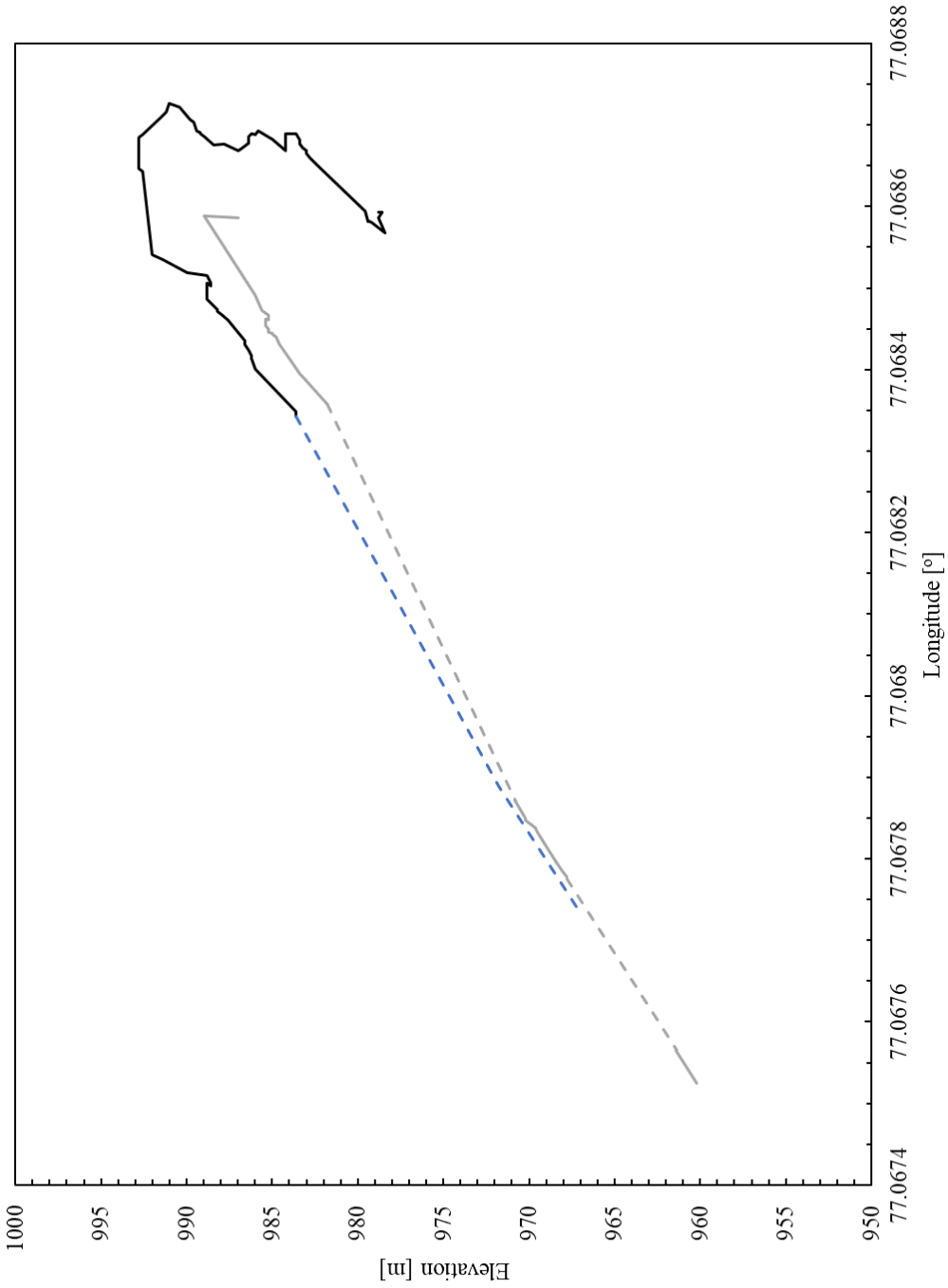

Figure 2.13: *GPS coordinates (elevation and longitude) of the top and toe of the headscarp of the largest Idukki landslide that was investigated. Dashed lines represent interpolated landslide extents.*

Figure 2.14: *Photographs of the main headscarp of the largest landslide in Idukki (9.7964191°N; 77.0682762°E).*

Figure 2.15: *Photograph of one of the damaged houses within the Idukki Landslide. Using multiple photographs of this house, this geometry of this house was reconstructed using Photoscan (9.7962622°N; 77.0681814°E).*

(a)

(b)

Figure 2.16: *Three-dimensional reconstruction of one of the houses within the Idukki Landslide by means of Photoscan. (a) Front left isometric projection, (b) top left isometric projection (9.7962622°N; 77.0681814°E).*

Figure 2.17: *Left side isometric projection of the three-dimensional reconstruction of one of the houses within the Idukki Landslide by means of Photoscan (9.7962622°N; 77.0681814°E).*

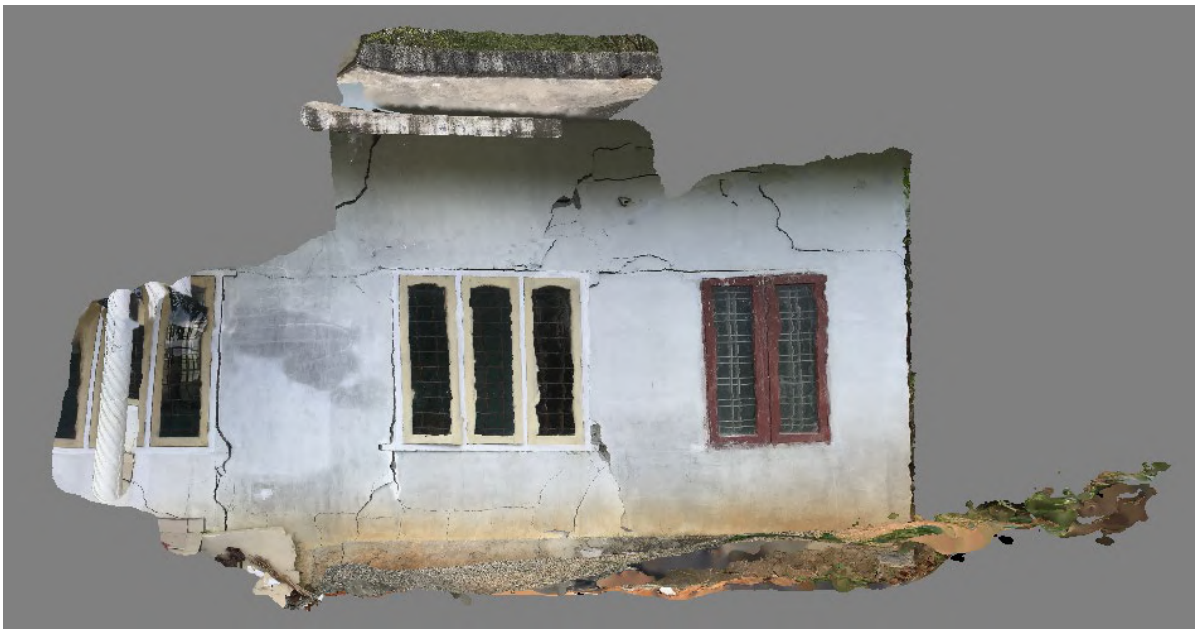

(a)

(b)

Figure 2.18: *Three-dimensional reconstruction of one of the houses within the Idukki Landslide by means of Photoscan. (a) Front right side isometric projection, (b) top right side isometric projection (9.7962622°N; 77.0681814°E).*

Chapter 3 - Dams and Reservoirs

Introduction

The State of Kerala, India has over major 45 dams and reservoirs (Wikipedia contributors, 2018). Around 22 major rivers contribute water to these reservoirs. The geographic location and brief detail of the dams and reservoirs are presented in Table-3.1. Most of these reservoirs are multi-objective with power generation and irrigation being the main outcome. The August 2018 rain and floods forced the authorities to open 35 of the large dams. The initial evidences suggest that the intensity of Kerala floods could have been reduced if the water from 35 large dams was released earlier based on the weather forecasts. Generally, the dams and their auxiliary structures performed satisfactorily during the august 2018 floods, with the exception of Maniyar dam in Pathanamthitta district that had some damage. The GEER team visited two of the dams. Due to restrictions for photography at dam's sites, the GEER team was not able to photograph the observations but rely on published pictures and satellite images. The two dams that the GEER team visited are Kallarkutty dam in Idukki district and Idamalayar dam in Ernakulam district. This chapter would provide a brief description of the two dams that the GEER team visited and Maniyar dam that experienced some damage.

Table 3.1: The list of major dams and their locations in Kerala (Source: modified from Wikipedia contributors, 2018)

SI: No	River	Name	Area (km^2)	District	Co-ordinate	Altitude (m)
1	Bharathapuzha River	Malampuzha Dam	23.13	Palakkad	10.84°N 76.69°E	104
2	Bharathapuzha River	Mangalam Dam	3.93	Palakkad	10.51°N 76.54°E	72
3	Bharathapuzha River	Meenkara Dam	2.59	Palakkad	10.62°N 76.80°E	152
4	Bharathapuzha River	Chulliar Dam	1.59	Palakkad	10.59°N 76.77°E	143
5	Bharathapuzha River	Pothundi Dam	3.63	Palakkad	10.54°N 76.63°E	93
6	Bharathapuzha River	Walayar Dam	2.59	Palakkad	10.84°N 76.86°E	197
7	Bharathapuzha River	Kanjirapuzha Dam	5.12	Palakkad	10.98°N 76.55°E	90
8	Chalakkudy River	Parambikulam	20.92	Palakkad	10.39°N 76.8°E	545
9	Chalakkudy River	Thunakkadavu Dam	2.83	Palakkad	10.433°N 76.784°E	565
10	Chalakkudy River	Peruvaaripallam Dam	0.65	Palakkad	10.447°N 76.77°E	27.74
11	Chalakkudy River	Sholayar Dam	8.70	Thrissur	10° 17' 76° 45'	

12	Chalakkudy River	Peringalkuthu Dam	2.63	Thrissur		
13	Chelakkara River	Asurankund Dam		Thrissur	10.6855° N, 76.2955° E	
14	Erattayar Lake	Erattayar Dam		Idukki		
15	Kabini River	Banasura Sagar Dam		Wayanad		
16	Kakkattar River	Maniyar Dam		Pathanamthitta	9.329203° N, 76.880749° E	
17	Kallada River	Thenmala Dam	25.90	Kollam	09° 57' 77° 4'20"	
18	Karamana River	Aruvikkara Dam	2.58	Thiruvananthapuram	08° 28' 77° 58'	
19	Karamana River	Peppara Dam	5.82	Thiruvananthapuram		
20	Karapuzha River	Karapuzha Dam		Wayanad		
21	Karuvanoor River	Peechi Dam	12.63	Thrissur	10.53°N 76.39°E	73
22	Keecheri River	Vazhani Dam	2.55	Thrissur	10° 40' 76° 15'	
23	Kurumali River	Chimmony Dam	8.51	Thrissur	10.4391°N 76.4604°E	
24	Kuttiady River	Kuttiady Dam	10.52	Kozhikode	11° 36' 75° 49'27"	
25	Kuttiyadi River	Kakkayam Dam	7.15	Kozhikode		
26	Muvattupuzha River	Malankara Dam	11.00	Idukki		
27	Neyyar River	Neyyar	15.00	Thiruvananthapuram	08° 32' 77° 08'	
28	Pamba River	Pamba Dam	5.70	Pathanamthitta	09° 20' 76° 53'	
29	Pamba River	Kakki	18.00	Pathanamthitta	9°17′N 77°15′E	981
30	Periyar River	Idukki Dam	61.60	Idukki	09° 48' 76° 53'	720
31	Periyar River	Ponmudi Dam	2.60	Idukki	09° 55' 77° 05'	
32	Periyar River	Anayirankal Dam	4.33	Idukki	10° 0' 77° 0'	
33	Periyar River	Kundala Dam	2.30	Idukki	10° 0' 77° 0'	
34	Periyar River	Mattupatti Dam	3.24	Idukki	10° 05' 77° 05'	
35	Periyar River	Sengulam Dam	0.33	Idukki	10° 00' 77° 05'	
36	Periyar River	Neriamangalam Dam	4.13	Ernakulam		
37	Periyar River	Bhoothathankettu Dam	6.08	Ernakulam		
38	Periyar River	Periyar Lake	28.90	Idukki	10° 10' 76° 15'	
39	Periyar River	Mullaperiyar Dam		Idukki		
40	Periyar River	Cheruthoni Dam		Idukki		
41	Periyar River	Kulamavu Dam		Idukki		
42	Siruvani River	Siruvani Dam		Palakkad		
43	Valapattanam River	Pazhassi Dam	6.48	Kannur		
44	Idamalayar River	Idamalayar Dam	28.3	Idukki	$10^0$13’ 15” N, longitude 76^0 : 42’: 30” E	102.80
45	Mudira Puzha	Kallarkutty Dam	0.64	Idukki		43

Select Dam Cases

Idamalayar Dam: The Idamalayar dam is gravity concrete structure with a length of 373m at the crest and 102.80m height. The location of Idamalayar dam and reservoir is shown in Figure 3.1. Figure 3.2 shows a downstream and upstream view of the dam. Idamalayar dam was commissioned in 1987. The dam and the reservoir is used for power generation. The water from the reservoir is transported through tunnel, surge shaft, penstocks to the power station that is 1700 m away from the reservoir. The surface power station produces around 75 MW of power from the reservoir. The shutters of the Idamalayar dam was open on August 9th at 5 am as the reservoir hit its full capacity of 169 meters (Figure 3.3).

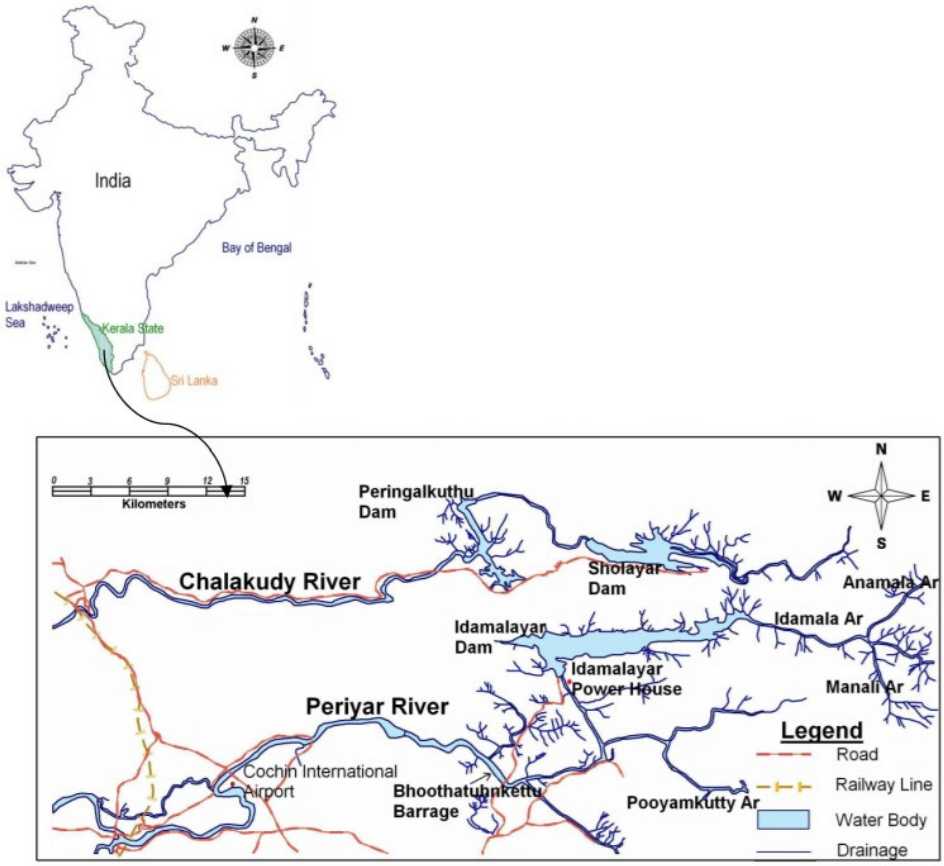

Figure 3.1: Location map showing the Idamalayar dam and reservoir. Source: Abe &James (2013).

Figure 3.2: Downstream and upstream view of the Idamalayar dam. Source Wikipedia contributors, 2018)

Figure 3.3: Shutters of Idamalayar dam in Kerala opened as reservoir hits full capacity source: The News Minute

During the visit to the Idamalayar dam site, the GEER team noticed that there are some landslides and rock fall occurring downstream of the reservoir close to the dam. It was evident that these landslides had occurred from the recent opening of the shutters and the heavy flow of the water had under-cut the banks of the downstream channel. The GEER team was not allowed to take photographs at the dam sites and therefore, couldn't document it.

However, looking at the available high-resolution satellite images from Planet lab indicates that these landslides were formed after the opening of the shutters. Figure 3.4 is a planet lab imagery of Idamalayar dam from July 1, 2018. It is evident from the image that the dam shutter is closed and the downstream channel is vegetated. Figure 3.5 is a planet lab imagery of Idamalayar dam on September 3rd, 2018 and it documents the landslides that are occurring in the downstream channel at close vicinity of the dam. The initial estimates indicate that the landslide is occurring less than 150m downstream of the dam. The width of the slide is roughly 100m.

Figure 3.4: Planet lab imagery of Idamalayar dam from July 1, 2018.

Figure 3.5: Planet lab imagery of Idamalayar dam from September 3, 2018.

Kallarkutty Dam: The Kallarkutty dam is located in Idukki district (Figure 3.6). The Kallarkutty dam was constructed in 1961 and is a masonry gravity dam with a length of 182.88m. The height of the dam is 43m. The dam has five spillways with gates of 10.97m x 6.40m. The Kallarkutty dam provides the reservoir for power generation at Neriamangalam powerhouse. The dam intercepts water from the Mudirapuzha River, which is a major tributary of the Periyar River. It was reported by the news media that the Kallarkutty dam overflowed on August 14th 2018. The GEER team visited the dam site and didn't see any visible signs of distress or damage from the overflow.

Figure 3.6: Location of Kallarkutty dam in Idukki District (9°19'20"N 76°52'30"E).

Maniyar Dam: The Maniyar Dam is located in Pathanamthitta District of Kerala (Figure 3.7). The Maniyar dam was constructed in 1993 and is a masonry gravity dam with a length of 115.22m. The height of the dam is 16.76m. The dam has five spillways with gates of 10.7m x 5.5m. The Maniyar Dam is used for power generation and is owned by Carborundum Universal Murugappa Limited CUMI, which is a tripartite collaboration between Murugappa Group, Carborundum Company USA & Universal Grinding Wheel Company UK. The dam intercepts water from the Kakkad River which is a major tributary of the Pampa River. It was reported by the news media that the Maniyar dam experienced some damage during the August 2018 floods. The GEER team was not given permission to visit the Maniyar Dam site. However, looking at Instagram pictures and news reports the GEER team has documented the damages at Maniyar Dam.

Figure 3.7: Location of Maniyar Dam in Pathanamthitta District (9.329203° N, 76.880749° E).

Reviewing the photographs from Instagram shows that the downstream side of the Maniyar dam beside the retaining structure has experienced some failure between August 10th and the 25th, 2018 (Figure 3.8). A closer view of the slope failure obtained from onmanorama indicate that the slope and the retaining structure had failed and material was eroded away (Figure 3.9). It is also evident from these photographs that there is some seepage occurring at the location where the slope failed. It is not clear whether this is seepage of groundwater or water from the upstream reservoir. From the pictures (Figure 3.10 & 3.11), it is also evident that the downstream side of the shutter-2 has experienced damage and the surface blocks have been displaced.

Figure 3.8: (Left) Downstream side of the Maniyar Dam with the shutters open on August 10th. (Right) Similar view as the left image taken on August 25th showing minor slope failure and damage to the retaining structure (failures are circled in red). Source of photograph: Instagram

Figure 3.9: Closer view of the slope failure and seepage at the downstream side of the Maniyar dam (Source: manoramaonline.com).

Figure 3.10: Photograph showing one shutter of the dam being closed and the surface concrete blocks been damaged (Source: manoramaonline.com).

Figure 3.11: Different view of the damage to the downstream surface of shutter-2 at Maniyar Dam (Source: manoramaonline.com).

Summary of Performance of Dams

The State of Kerala, India has over major 45 dams and reservoirs and most of them are used for hydroelectric production. The GEER team only visited two of the dams and was not given permission for photography. At the Idamalayar Dam site, the GEER team observed a landslide very close to the dam that needs to be carefully monitored and studied to investigate whether it has any impact on the integrity of the dam. The size and location of the landslide was verified by the GEER team using satellite images. The Kallarkutty Dam performed well even though there was news that it overflowed. No signs of visible damage were observed at the Kallarkutty Dam. The analysis of instagram and news media pictures indicate that Maniyar Dam has experienced some damages to the Shutter-2 and the retaining wall. There is also visible sign of seepage. These damages need to be investigated to evaluate the stability of Maniyar Dam. An Unmanned Aircraft Vehicle (UAV) based analysis using thermal and optical sensors can be a useful approach to document the condition of the dams (Brooks et al. 2015; Oommen et al. 2019).

The opening of the shutters of over 35 dams in Kerala during the peak of the rainfall event has further intensified the flooding in Kerala. Since most of the dams in Kerala are used for power generation, the authorities who maintain the dam wait till the maximum water level to open the shutter. Although this approach is ideal to maximize power generation, it needs to be reevaluated in the context of the 2018 August flood damage. To avoid such events in the future, an approach that maximizes power generation while incorporating weather prediction needs to be adopted for managing dams and reservoirs in Kerala.

Chapter 4 - Foundation Failures

Introduction

In the afternoon of September 4, 2018, while driving West from Alleppey along SH11 (also referred to as the Alappuzha-Changanassery [AC] Road or as the Alappuzha-Veliyanad Road), Dr. Thomas Oommen noticed a purple house (located at coordinates Latitude=9.4626^{o}, Longitude=76.3659^{o}) that was leaning (Figure 4.1). The house was located on the North side of the road just after passing the Pallathuruthy Bridge. After noticing the house, the GEER team, turned around and returned to the purple house to collect dynamic cone penetration (DCP) data at points surrounding the purple house. The team was onsite at the purple house location from 16:26 hours until 17:45 hours local time (GMT+5:30). While on site, the team collected three (3) DCP soundings. As shown in Figure 4.2, the soundings were located outside of the Northwest, Northeast, and Southcentral portions of the purple house. The data from the soundings for the DCP are reported in Figure 4.3. The team also returned to the location of the purple house at 08:30 hours on the morning of September 5, 2018, to determine what construction practices were used to construct the two-year old, single-story, tan house that was located directly next to the eight-year old, single-story, purple house.

Select Locations:

Based on conversations with the residents, the foundation of the purple house consisted of an 18-inch wide by 4-inch thick reinforced concrete spread footing pad at a depth of 5-feet below ground surface with a 6-inch thick brick-masonry stem-wall placed on top of the spread footing. The aforementioned spread footing was constructed on top of rubble fill material. The walls of the purple house were made from brick masonry. The tan house that was constructed next to the purple house was also constructed on a spread footing that was constructed at a depth of approximately 5-feet deep. The tan house was also constructed with brick and masonry construction. However, unlike the purple house that was observed to have an asbestos roof, the tan house was observed to have a concrete roof (the color contrast of the various roof types is evident in the aerial photograph that was shown previously as Figure 4.2).

Figure 4.1: *Photograph of the subsided purple house located at coordinates Latitude=9.4626^{o}, Longitude=76.3659^{o}.*

As previously mentioned, the Northwest corner of the purple house was observed to have settled. However, direct measurement of the amount of settlement was not available due to 1) cost constraints associated with airline baggage restrictions preventing transport of a four-foot long level or total station and 2) the flood waters presenting a health hazard. Therefore, the tilt of the foundation was not measured by manual means. Instead 12 photographs of the purple house were acquired from multiple vantage points that were acquired from safe distances away from the flood waters. Post-processing of the photographs in PhotoModeler (PhotoModeler, 2018) and PhotoScan (PhotoScan, 2018) software packages yielded differing results. As shown in Figure 4.4, a more dense point cloud was obtained from the PhotoScan software program than from the PhotoModeler software program. This finding surprised Dr. Coffman because of previous success by the group

at the University of Arkansas using the Photomodeler software and not PhotoScan software to reconstruct three-dimensional shapes of triaxial samples using close-range photogrammetry inside of a triaxial cell (Salazar and Coffman 2015a, 2015b, Salazar et al. 2015, Salazar et al. 2017, Salazar 2017, Salazar et al. 2018).

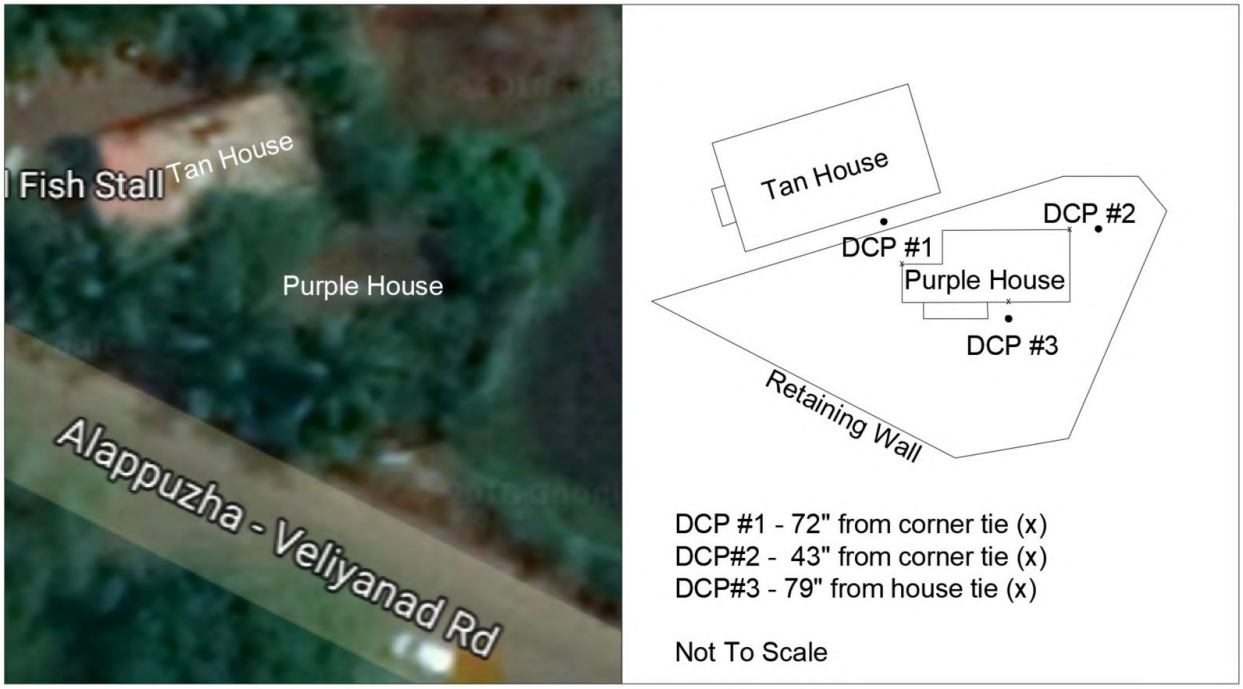

(a) (b)

Figure 4.2: *a) Google Maps (2018) image of the Tan/Purple Houses and b) a schematic of the relative locations of the DCP point locations.*

Following development of the three-dimensional point cloud data in PhotoScan (Figure 4.5), the three-dimensional point cloud data were extracted from the PhotoScan software. The point cloud data were then imported into the open-source program CloudCompare (2018) to determine the amount of differential settlement of the corner of the purple house. By using the point cloud points associated with the water surface as a datum, the North wall of the purple house was observed to have rotated by 1.7^{o} and the West wall of the purple house was observed to have rotated by 2.0^{o}.

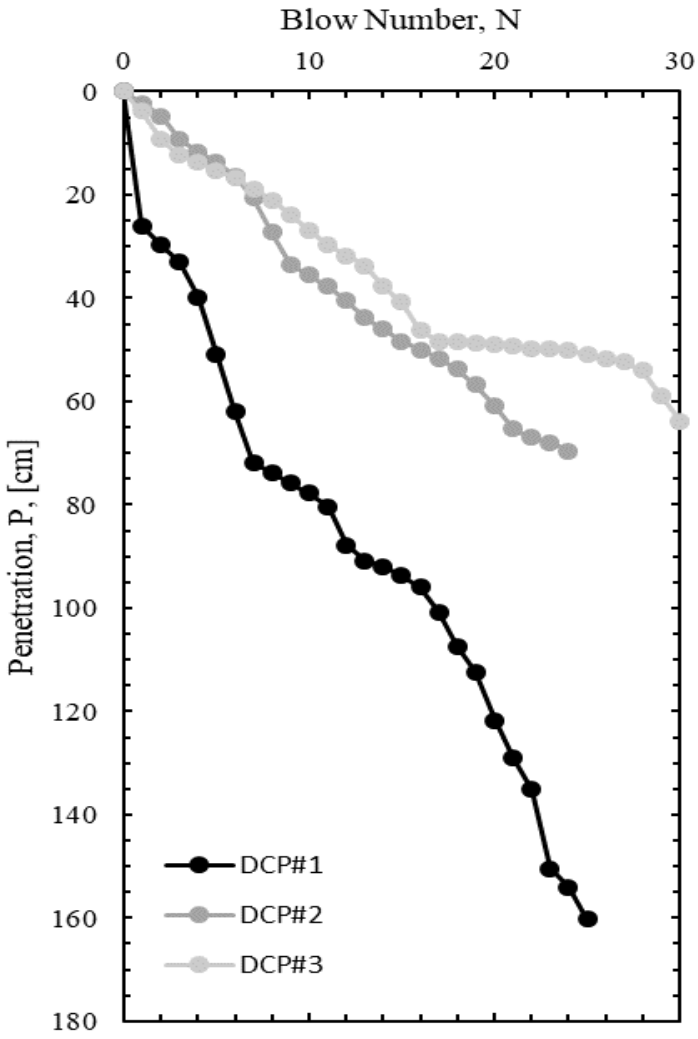

Figure 4.3: *DCP sounding data for the three (3) DCP soundings at the purple house.*

As shown in Figure 4.3, the lowest blow counts values were observed near the sunken corner of the purple house (DCP#1). However, as shown previously in Figure 4.2, the DCP#1 test was also collected near the central portion of the newer tan house. This observation, of the proximity of the DCP sounding to both houses, led to the following question: why was there differential settlement of the purple house but no differential settlement of the tan house? The rational for the corner of the purple house settling and rotating while the tan house did not settle nor rotate are listed below.

1) The stresses at the Northeast corner of the purple house were greater than the stresses along the South wall of the tan house. Even though the tan house has a concrete roof and thereby higher bearing pressures, the pressures at the location of DCP#1 were low for the tan house but high for the purple house.

2) The construction techniques for the tan house (concrete roof on concrete beams) as opposed to those for the purple house (asbestos roof on masonry walls). The concrete beams of the tan house appeared to have tied the tan structure together better than the masonry walls of the purple house.

Based on the observations from the purple and tan houses, the GEER team sought out other houses or building that may have experienced similar behavior. Although other structures were observed to have encountered subsidence induced settlement (e.g. Figure 4.7), the morning of September 5, 2018, was spent at two newly constructed two-story houses. These concrete roof on concrete beam houses were constructed following similar procedures to the aforementioned tan house. The houses were located directly across SH11 from the Mar Sleeva Church of Ponga. As shown in Figure 4.8, the two story houses and the Mar Sleeva Church of Ponga that were investigated on September 5 were located approximately 1.83 miles Southeast of the aforementioned tan and purple houses along SH11 (also referred to as the Alappuzha-Chanfanassery [AC] Road or as the Alappuzha-Veliyanad Road).

Photographs of the two-story houses (identified as the white and gray houses) are shown in Figure 4.9. Based on conversations with the residents of the homes, the second story of the white house was constructed from lightweight concrete and the gray house was constructed on a mat foundation. For completeness, photographs of the blue prints for this house, which were provided by the owner of the house, are included as Figure 4.10. The residents also stated that the original building of the Mar Sleeva Church (Figure 4.11), located across SH11 from the houses, was constructed on 30-foot long concrete piles and the ancillary building was constructed on six- to eight-foot long sections of coconut trees placed in nine-pile groups. The location of the DCP soundings around the white and tan two story homes are provided in Figure 4.12. The DCP sounding data from the four soundings that were performed at this site are provided in Figure 4.13.

Likewise, for comparative purposes, these soundings are compared against the sounding from the purple house.

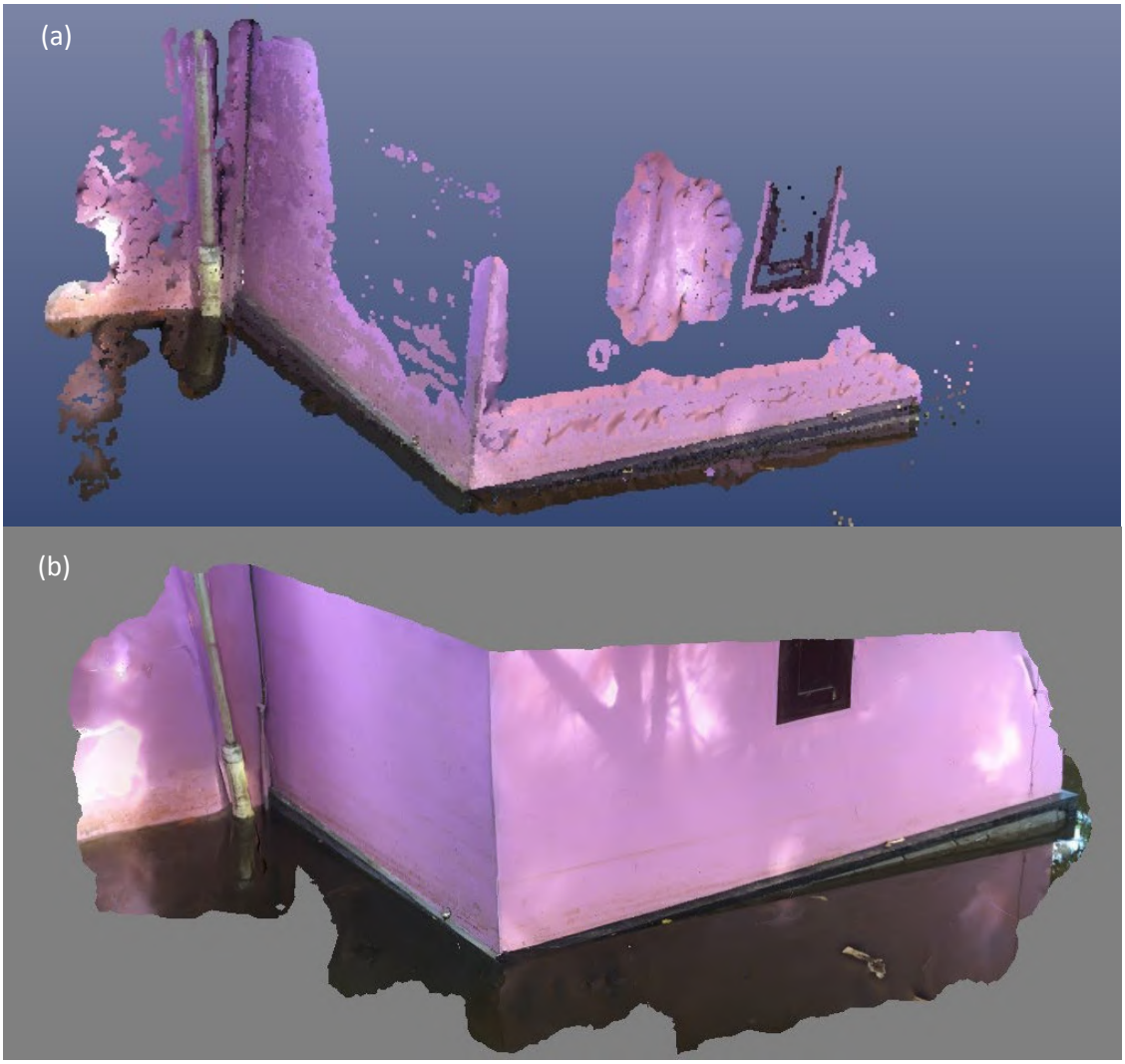

Figure 4.4: *a) PhotoModeler and b) PhotoScan renderings of draped images overlain on the three-dimensional point cloud data that were developed from the 12 acquired photographs with different viewing angles.*

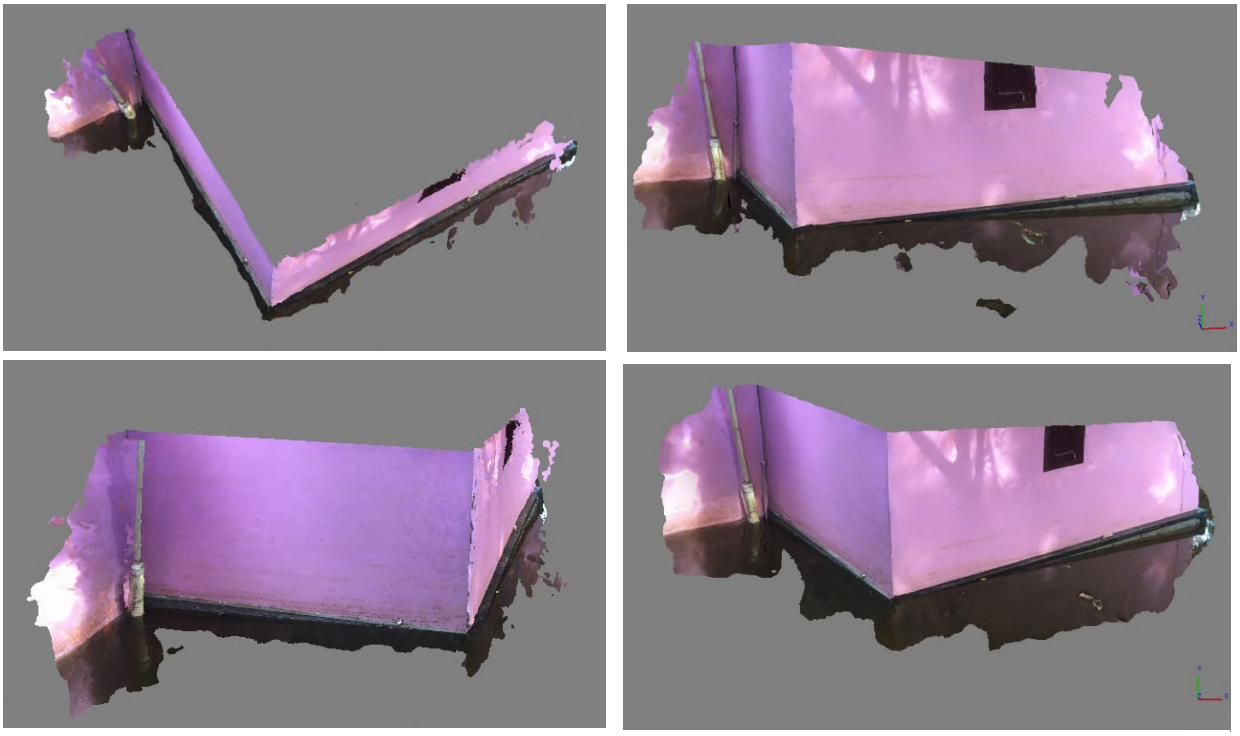

Figure 4.5: *Multiple views of PhotoScan renderings of draped images overlaid on the three-dimensional point cloud data that were developed from the 12 photographs acquired from different viewing angles.*

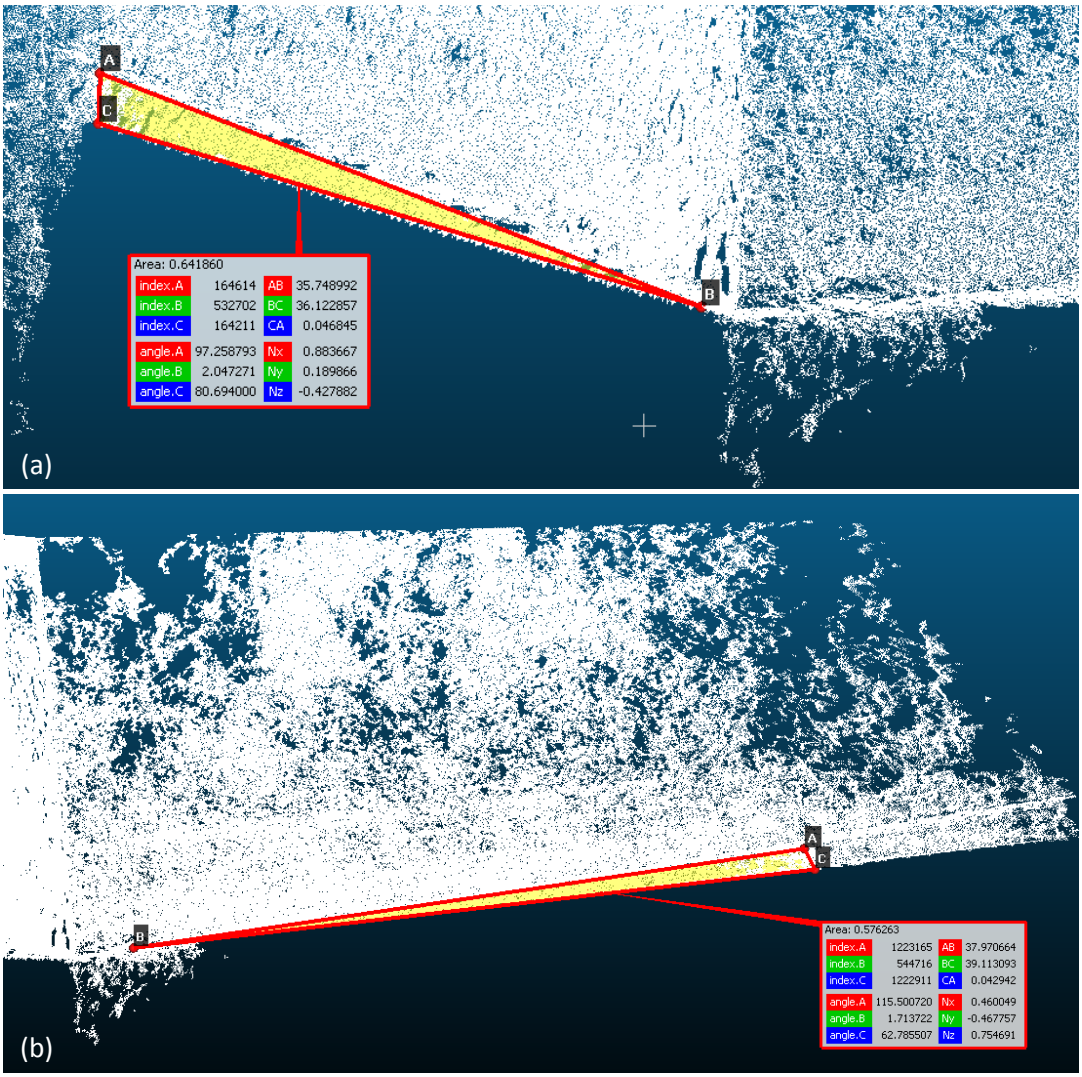

Figure 4.6: *PhotoScan rendering of three-dimensional point cloud data used to determine rotation of the foundation associated with differential settlement for a) North wall (1.7^o tilt), b) West Wall (2.0^o tilt).*

***Figure 4.7**: Photograph of building that tilted due to differential settlement following floodwater withdrawal (Latitude=9.453415^o, Longitude=76.385143^o).*

***Figure 4.8:** a) Google Maps (2018) image showing the 1.83 mile distance between the Kumbam Velil Fish Stall (location of single-story tan and purple houses) and the Mar Sleeva Church of Ponga (location of church and two-story concrete homes).*

Figure 4.9: *Photographs of the a) white and b) gray houses located across from the Mar Sleeva Church. Photograph of white house provided by Thomas Mampra.*

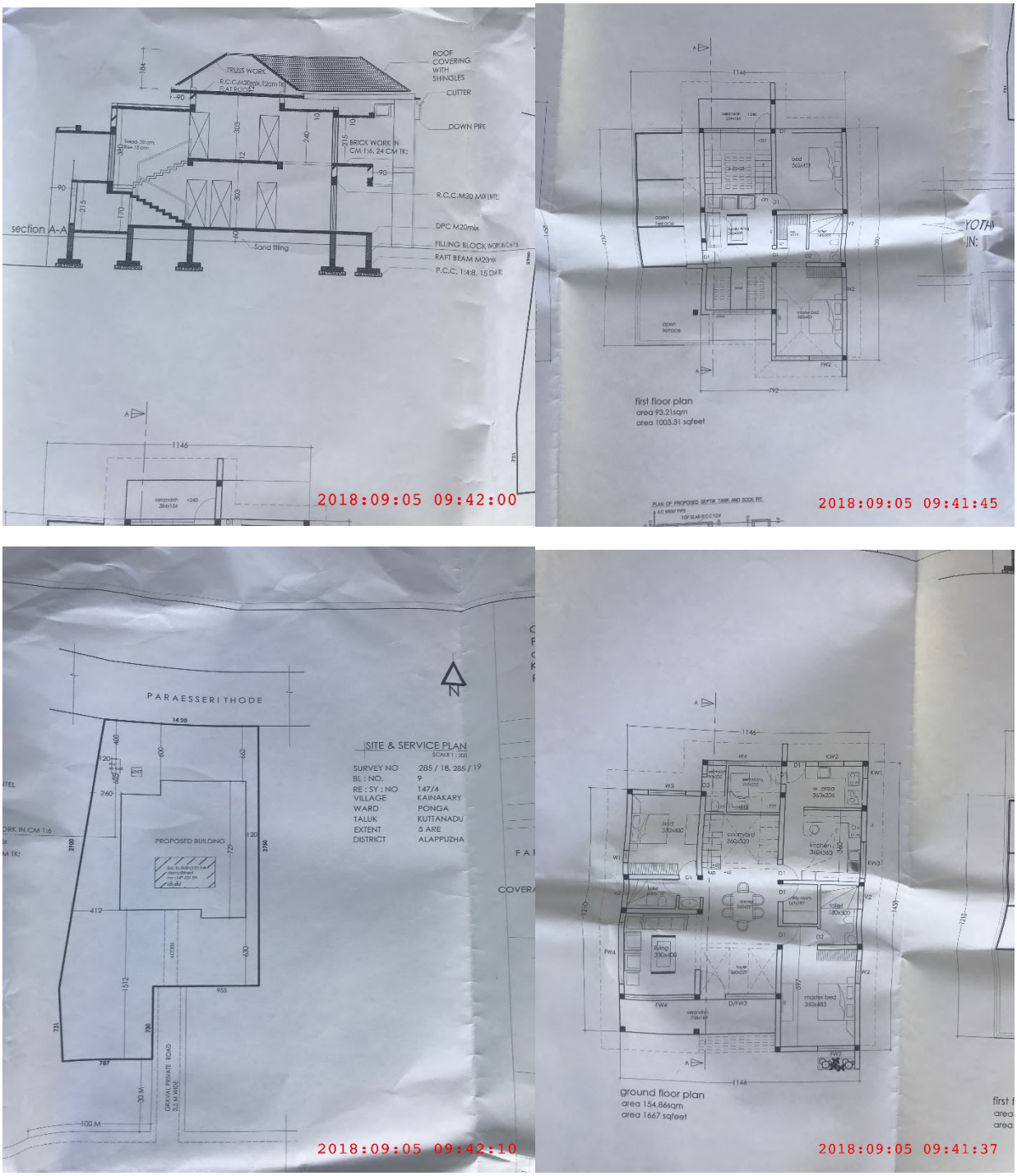

Figure 4.10: *Blue prints of the house surveyed @ 9.4507908^{0}N; 76.3906122^{0}E*

Figure 4.11: *Mar Sleeva Church. Original Church constructed on 30-foot long concrete piles; ancillary building constructed on six- to eight-foot long sections of coconut trees placed in nine-pile groups (Latitude=9.450352º, Longitude=76.389449º).*

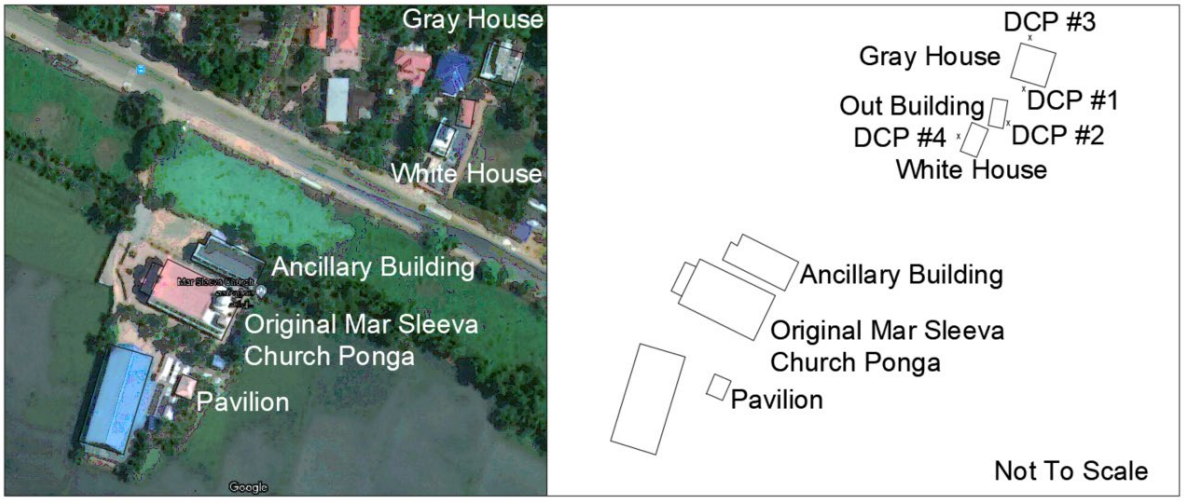

(a) (b)

Figure 4.12: *a) Google Maps (2018) image of the Mar Sleeva Church and the White/Gray houses, and b) a schematic of the relative locations of the DCP point locations near the White/Gray houses.*

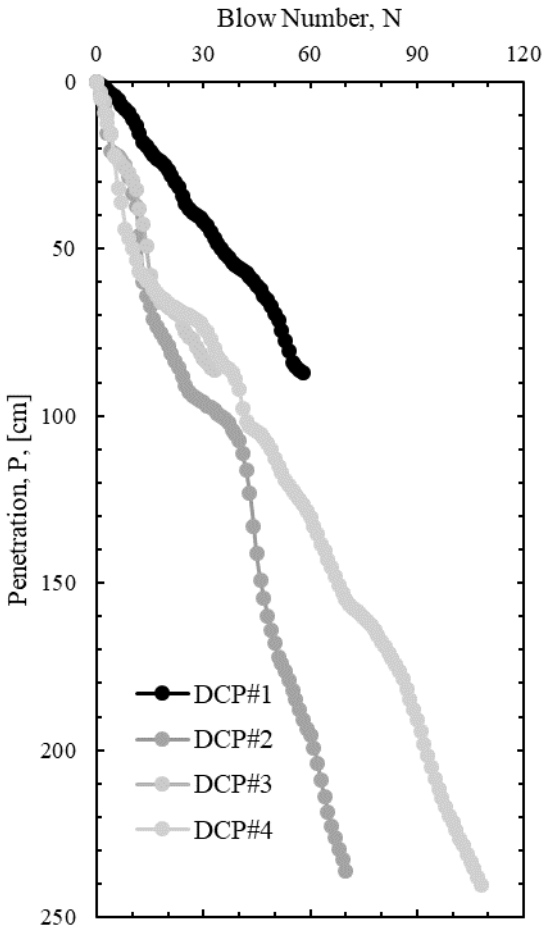

Figure 4.13: *DCP sounding data for the four (4) DCP soundings at the white/gray house.*

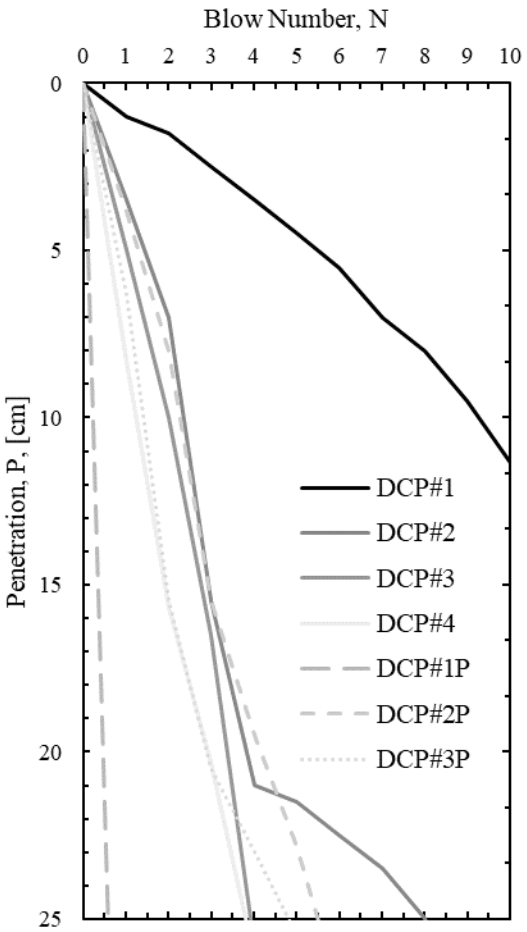

Figure 4.14: *DCP soundings at the white/gray houses compared with those at the purple (P)/tan houses.*

By comparing the data in Figure 4.14, it is apparent that the strength of the soil located at the Northwest corner of the purple house was significantly weaker than all of the other soundings. It was also apparent that the soil located outside of the front door of the Gray house was significantly stronger than all of the other soils. The reminder of the soils were comparable for the first 25cm. It is fitting that all of the other soil strengths were similar because all of these other soils were comprised of agricultural rice patty soils except for the sounding located next to the white house that was driven through approximately one-foot of fill material. Based on the similarity of the observed strengths, these soils were most likely borrow soils from a nearby area.

As observed in the photograph in Figure 4.15, the above burial ground pavilion at Mar Sleeva Church Ponga rotated like the purple house and business that were previously mentioned. Like the differential settlement associated with the purple house, the differential settlement of the pavilion was believed to be caused by differential stresses. Specifically, the rotation was believed to be caused by the differential loading associated with the back wall shown in Figure 4.15 causing high stresses on the foundation at the back of the Pavilion that were not counter balanced with a front wall on the pavilion. The flooding water levels, at the Mar Sleeva Church are represented by means of comparison between the photographs shown in Figures 4.11 and 4.14. The water level during flooding was observed to reach the doorway of the church (Figure 4.16) and was high enough to ruin the carpet inside of the church and the electrical wiring that was spread across the floor of the church. These items were being replaced in the church during the GEER visit.

Although no structural rotations were observed to occur in the buildings constructed on piles (Mar Sleeva Church Ponga and ancillary building), cracking was observed in the back wall of the church (Figure 4.17) and differential settlement was observed between the church and the surrounding concrete pavers (Figure 4.18). Because the surrounding pavers were observed to be lower than the previous position of the pavers, as indicated by markings on the steps of the church, it is believed that the surrounding soil subsided while the church remained relatively stationary. It is important to note that cracking occurred in the back wall (East wall) and this was the same side (East side) that the rotation occurred for the pavilion that was located nearby. Although unsubstantiated, it is believed that the back one-story portion of the building was not constructed on piles like the

remainder of the church. This difference in rigidity between the different portions of the building led to the observed cracks. The neighbors in the white and gray houses indicated that a geotechnical investigation was performed prior to pile driving. The GEER team is obtaining the report for the geotechnical investigation.

Figure 4.15: *Photograph of rotated pavilion located behind the Mar Sleeva Church of Ponga (Latitude=9.449777°, Longitude=76.389598°).*

Figure 4.16: *Photograph of the Mar Sleeva Church Ponga when subjected to flooding. Gray house and white house identified in background. Photograph provided by Mar Sleeva Church Ponga.*

Figure 4.17: *Photograph of cracking observed within the back wall of the Mar Sleeva Church or Ponga.*

Figure 4.18: *Photograph of cracking occurring in the concrete pavers surrounding the pile supported Mar Sleeva Church of Ponga building.*

Chapter 5 - Other Impacts

Introduction

The Kuttanad region of Alleppey district is the only place in India that cultivates rice below the sea level. The Location of Kuttanad in Alleppey district is shown in Figure 5.1. In Kuttanad, three landscape elements are used for rice cultivation. These elements are the Karapadam (upland rice fields), Kayal (wetland rice fields), and Kari (land buried with black coal like material).

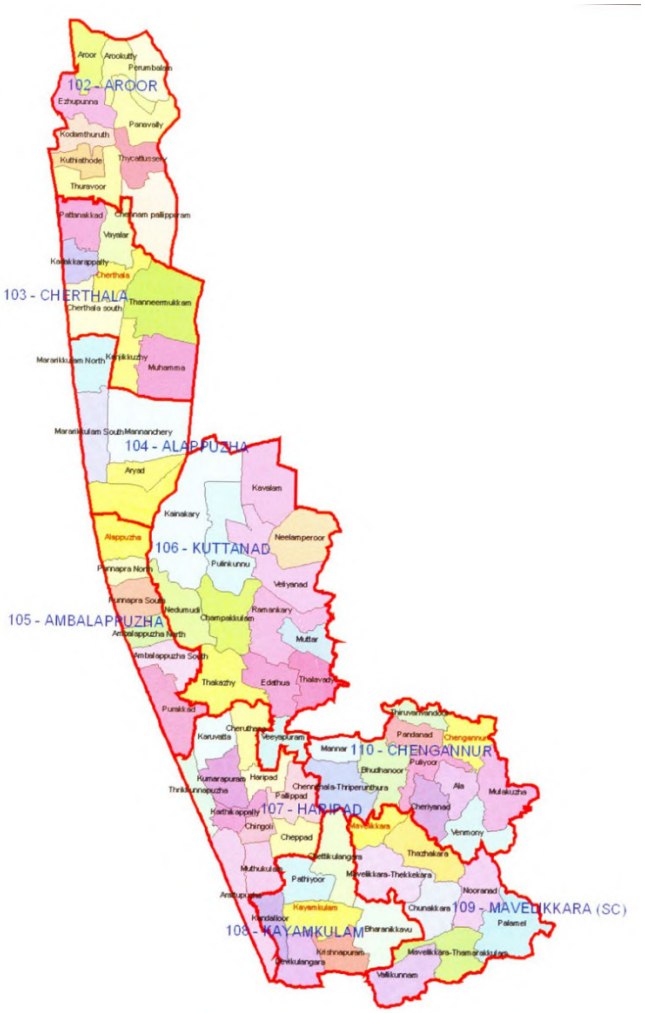

Figure 5.1: District map of Alleppey showing the region of Kuttanad. Source: newalliedtour.net

Typically, the Kayal/wetland rice fields are separated from the lake with a bund/ embankment with coconut trees grown on these bunds (Figure 5.2). The cultivation of rice below sea level in Kuttanad was developed by the local farmers and has several similarities with the Dutch polder system (MSSRF, 2007). On the Kayal side, the farmers build their house on a filed piece of land or a natural elevated land as shown in Figure 5.3.

Figure 5.2: Coconut trees on the bund that separate the Vembanad Lake (on the left of bund) from the Kayal (on right of bund). Source: www.fao.org/3/a-bp793e.pdf

The wetlands are usually 0.60m to 2.0m below the Mean Sea Level (MSL) and are abundant with sand, silts, and organics. The wetlands extend about 9400 hectare area protected by bunds that are up to a 1.0m above the MSL (MSSRF, 2007). The wetlands are mostly land obtained by reclamation from the Vembanad Lake, which is the longest lake in India. The land was reclaimed by identifying vast stretches of shallow land in the lake and marking them by bamboo poles. Once the land is marked out, the bund construction begins. The bund was constructed by driving coconut tree poles deep into the lake that are closely spaced. Once the first row of coconut tree poles are completed, a second row is started at a distance of 1.5 to 3m parallel to the first row. The bracing

Figure 5.3: On the foreground is the lake and on the background of the house is the wetland rice fields (Kayal).

and protection of the coconut poles are achieved using woven coconut leaves and aracnut tree poles. The space between the two rows of coconut poles will then be filled with rice straw reinforced clay. The properties of the clay are given in Table 5.1 (source: Greeshma & Joseph 2011).

Table 5.1: Properties of the Kuttanad clay used for bund construction (Source: Greeshma & Joseph 2011).

Properties	Kuttanad clay
Sand content (%)	8
Silt size content (%)	52
Clay size content (%)	40
Specific Gravity	2.04
Liquid Limit (%)	100
Plastic Limit (%)	36
Plasticity Index (%)	64
Optimum moisture content (%)	33.0
Maximum dry density(kN/m^3)	13.6
Unconfined compressive strength(kPa)	21.09

Greeshma and Joseph (2011) verified that the rice straw reinforcement of the clay provided 1.94 times more unconfined compressive strength compared to the unreinforced clay.

Impacts of the August 2018 Floods on the Bund

The August 2018 flood resulted in the collapse of bund at several locations. Apart from the heavy rainfall and opening of shutters of almost all major dams, it was high tide time in the Arabian Sea and therefore, flood water could not get discharged. Most of the bund collapse were minor and could be fixed in couple days (Figure 5.4). However, one major failure of the bund occurred near Kainakari (@ 9.5029947^0N 76.3749555^0E) (Figure 5.5). This caused the water from the river to enter the below MSL Kuttanad area and these areas remain inundated even during the GEER team visit (roughly 12-15 days after the rain event) (Figures 5.6, 5.7, & 5.8).

Figure 5.4: A minor bund failure @ 9.5032131^0N 76.3768638^0E.

Figure 5.5: A major bund failure of roughly 50m long near Kainakari @ 9.5029947^{0}N 76.3749555^{0}E. The left side of the bund in the photograph is the lake and the right side of the bund is the flooded fields.

Figure 5.6: Flooded temple complex from the bund failure @ 9.5033596^{0}N 76.3771085^{0}E

Figure 5.7: Flooded community hall from the bund failure @ 9.5033444^{0}N 76.3770758^{0}E

Figure 5.8: Entrance of the flooded community hall @ 9.5033389^0N 76.3772861^0E

Figure 5.9: Flooded home due to bund failure @ 9.5032691^0N 76.3776221^0E

The GEER team witnessed the reconstruction of the major bund failure. The reconstruction was labor intensive and was done using locally available construction material (Figure 5.5). The government had taken measures to pump the water from the flooded fields as the bund was being reconstructed as shown in Figure 5.10.

Figure 5.10: Water being pumped from the fields to the lake @ 9.5166260^{0}N 76.3810643^{0}E

References

Abe, G., & James, E. J. (2013). Flood moderation by large reservoirs in the humid tropics of Western Ghat region of Kerala, India. Journal homepage: www. IJEE. IEEFoundation. org, 4(1), 141-152.

Anbazhagan, S., Sajinkumar, K.S. (2011) Geoinformatics in terrain analysis and landslide susceptibility mapping in parts of Western Ghats, India. In: Anbazhagan S, Subramaniam SK, Yang X (Eds), Geoinformatics in Applied Geomorphology, CRC Press, pp.291-315

Bíl, M., Andrásik, R., Zahradnícek, P., Kubecek, J., Sedoník, J., Stepánek, P. (2015) Total water content thresholds for shallow landslides, Outer Western Carpathians. Landslides 13 (2), 337-347.

Bouali, E. H., Oommen, T., & Escobar-Wolf, R. (2016). Interferometric stacking toward geohazard identification and geotechnical asset monitoring. Journal of Infrastructure Systems, 22(2), 05016001.

Brooks, C., Dobson, R.J., Banach, D.M., Dean, D., Oommen, T., Wolf, R.E., Havens, T.C., Ahlborn, T.M. and Hart, B., (2015). Evaluating the use of unmanned aerial vehicles for transportation purposes (No. RC-1616).

CloudCompare (2018). "CloudCompare" <https://www.danielgm.net/cc/>. Accessed September 29, 2018.

Flood Management (2018) http://www.india-wris.nrsc.gov.in/wrpinfo/index.php?title=Main_Page

Greeshma, P. G., & Joseph, M. (2011). Rice straw reinforcement for improvement in Kuttanad clay. In Proceedings of the Indian Geotechnical Conference.

GSI (2005) Geology and Mineral Resources of Kerala 2nd Edition. Misc. Publ. Geol. Surv. India, no.30, pp.93.

In Just 20 Days, Kerala Gets Highest August Rains in 87 Years. (2018) The Weather Channel, The Weather Channel, www.weather.com/en-IN/india/monsoon/news/2018-08-21-kerala-august-rain.

Kannan K. P, (1979) 'Ecological and socio-economic consequences of water control', proceeding of Indian Academy of Science, vol. C2, part 4, pp. 417-433.

Kerala Geography & History (2018) My India, www.mapsofindia.com/maps/kerala/geography-and-history/.

Kerala Floods Claimed 483 Lives, 15 Still Missing: CM Pinarayi Vijayan." Https://Www.hindustantimes.com/, Hindustan Times, 30 Aug. 2018, www.hindustantimes.com/india-news/kerala-floods-claimed-483-lives-15-still-missing-cm-pinarayi-vijayan/story-8NILqFOSNOtA459rfjovCN.html.

Keyport, R. N., Oommen, T., Martha, T. R., Sajinkumar, K. S., & Gierke, J. S. (2018). A comparative analysis of pixel-and object-based detection of landslides from very high-resolution images. International Journal of Applied Earth Observation and Geoinformation, 64, 1-11.

Mampra, Thomas (2018). Facebook Post. https://www.facebook.com/photo.php?fbid=1344635289013888&set=pcb.1345273052283445&type=3&theater. Accessed October 1, 2018.

Mar Sleeva Church Ponga (2018). Facebook Post. https://www.facebook.com/sleevachurch/photos/a.404057569944923/676733036010707/?type=3&theater. Accessed October 1, 2018.

McDonnell JJ (1990) The influence of macropores on debris flow initiation. Q J Eng Geol 23:325–331

Montrasio, L., Valentino, R. (2007) Experimental analysis and modelling of shallow landslides. Landslides 4 (3), 291-296.

Narendra Prasad S, 1998, 'Conservation planning for the Western Ghats of Kerala: II: Assessment of habitat loss and degradation', Current Science, vol. 75, pp. 228-235

Odom, A.L. (1982) Isotopic age determinations of rock and mineral samples from the Kerala State of India. Final report UN Case No. 81-10084 (Unpubld.).

Oommen, T., Baise, L. G., Gens, R., Prakash, A., & Gupta, R. P. (2013). Documenting earthquake-induced liquefaction using satellite remote sensing image transformations. Environmental & Engineering Geoscience, 19(4), 303-318.

Oommen, T., Cobin, P. F., Gierke, J. S., & Sajinkumar, K. S. (2018). Significance of variable selection and scaling issues for probabilistic modeling of rainfall-induced landslide susceptibility. Spatial Information Research, 26(1), 21-31.

Oommen, T., Bouali, E. H., & Wolf, R. E. (2019). New Paradigm in Geotechnical Performance Monitoring Using Remote Sensing. In Geotechnical Design and Practice (pp. 195-201). Springer, Singapore.

PhotoModeler (2018). "PhotoModeler" < https://www.photomodeler.com/index.html>. Accessed September 29, 2018.

PhotoScan (2018). "Agisoft" < http://www.agisoft.com/>. Accessed September 29, 2018.

Pierson TC (1983) Soil pipes and slope stability. Q J Eng Geol 16:1–11

Radhakrishna, B.P. (2001) Geomorphic rejuvenation of the Indian Peninsula. In: Gunnell Y, Radhakrishna BP, editors. Sahyādri: the great escarpment of the Indian subcontinent. Bangalore, Geological Society of India. p.201–211.

Rajan, P.K., Santosh, M. and Ramachandran, K.K. (1984) Geochemistry and petrogenetic evolution of the diatexites of Central Kerala, India. Proc.Indian Acad. Sci. (Earth Planet Sci.) 93(1):57-69.

Sahoo, B. C., Oommen, T., Misra, D., & Newby, G. (2007). Using the one-dimensional S-transform as a discrimination tool in classification of hyperspectral images. Canadian Journal of Remote Sensing, 33(6), 551-560.

Salazar, S.E., Barnes, A.R., Miramontes, L.D., Bernhardt, M.L., Coffman, R.A., (2018). “Validation of an Internal Cameral Based Volume Determination System for Triaxial Testing.” Geotechnical Testing Journal. Manuscript Accepted for Publication, in Typesetting. doi: 10.1520/GTJ20170125.

Salazar, Sean E., (2017). “Development of an Internal Camera-Based Volume Determination System for Triaxial Testing.” Masters Thesis. University of Arkansas. December.

Salazar, S.E., Barnes, A.R., Coffman, R.A., (2017). “Closure to “Discussion of ‘Development of an Internal Camera-Based Volume Determination System for Triaxial Testing’ by S.E. Salazar, A. Barnes and R.A. Coffman” by A. Mehdizadeh, M.M. Disfani, R. Evans, A. Arulrajah and D.E.L. Ong.” Geotechnical Testing Journal. Vol 40, No. 1, pp. 47-51. doi: 10.1520/GTJ20160154.

Salazar, S.E., Barnes, A.R., Coffman, R.A., (2015). “Development of an Internal Camera Based Volume Determination System for Triaxial Testing.” Geotechnical Testing Journal. Vol. 38, No. 4, pp. 1-7. doi: 10.1520/GTJ20140249.

Salazar, S.E., Coffman, R.A., (2015a). “Discussion of A Photogrammetry-based Method to Measure Total and Local Volume Changes of Unsaturated Soils During Triaxial Testing by X. Zhang, L. Li, G. Chen, and R. Lytton.” Acta Geotechnica. Vol. 10, Issue 4, pp. 1-4. doi: 10.1007/s11440-015-0380-1.

Salazar, S.E., Coffman, R.A., (2015b). “Consideration of Internal Board Camera Optics for Triaxial Testing Applications.” Geotechnical Testing Journal. Vol. 38, No. 1, pp. 1-11. doi:10.1520/GTJ20140163.

Sajinkumar, K.S. (2005) Geoinformatics in landslide risk assessment and management in parts of Western Ghats, Central Kerala, South India. Ph.D. Thesis (Unpublished), IIT Bombay

Sajinkumar, K.S. and Anbazahagan, S. (2015) Geomorphic appraisal of landslides on the windward slope of Western Ghats, southern India. Natural Hazards, v.75(1), pp.953-973.

Sajinkumar KS, Anbazhagan S, Pradeepkumar AP, Rani VR (2011) Weathering and landslide occurrences in parts of Western Ghats, Kerala. J Geol Soc India 78(3):249–57.

Sajinkumar, K.S., Anbazhagan, S., Rani, V.R. and Muraleedharan, C. (2014a) A paradigm quantitative approach for a regional risk assessment and management in a few landslide prone hamlets along the windward slope of Western Ghats, India. Internat. Jour. Disaster Risk Reduction 7:142-153.

Sajinkumar, K.S., Sankar, G., Rani, V.R., Sundarajan, P. (2014b) Effect of quarrying on the slope stability of Banasuramala- an offshoot valley of Western Ghats, Wayanad, India. Environ. Earth Sci. 72(7): 2333-2344.

Sajinkumar, K.S. and Rani, V.R. (2015) Contrasting anthropogenically influenced landslides in two different terrain conditions in the southwestern part of Peninsular India. In: Lollino G. et al. (Eds.), Engineering Geology for Society and Territory, Volume 2, pp.1005-1010.

Sajinkumar, K.S., Castedo, R., Sundarajan, P. and Rani, V.R. (2015) Study of a partially failed landslide and delineation of piping phenomena by vertical electrical sounding (VES) in the Wayanad Plateau, Kerala, India. Natural Hazards, v.75(1), pp.755-778.

Sajinkumar, K. S., Oommen, T. (2018) Landslide Atlas of Kerala. Geological Society of India, Bangalore.

Santosh, M., Iyer, S.S. and Vasconcellos, M.B.A. (1987) Rare earth element geochemistry of the Munnar carbonatite, Central Kerala. Jour. Geol. Soc. India, 29:335-343.

Sarkar S (2011) Evolution of the Paglajhora slump valley in the Shiv Khola basin, the Darjeeling Himalaya, India. Geogr Polon 82(2):117–126

Shruti Naidu, Sajinkumar K.S., Oommen T., Anuja V.J., Rinu A. Samuel, Muraleedharan C. (2018) Early warning system for shallow landslides using rainfall threshold and slope stability analysis. Geoscience Frontiers. https://doi.org/10.1016/j.gsf.2017.10.008

Simon S, Jacob, K. P, 2013, 'energy optimised secure routing protocol for wireless sensors' international journal of engineering and innovative technology, vol. 3, pp 72-79

Smith, D.M., Oommen, T., Bowman, T., Gierke, J.S., Vitton, S.J., 2015. Hazard assessment of rainfall-induced landslides: a case study of San Vicente volcano in central El Salvador. Natural Hazards 75 (3), 2291-2310.

Sundarajan, P. and Sajinkumar, K.S. (2012) Detailed site specific study of Narippara landslide, Wayanad district, Kerala. Geol. Surv. India, unpublished report

Thampi, P.K., Mathai, J., Sankar, G. (1995) Landslides (UrulPottal) in Western Ghats: Some field observations. In: Proceedings of seventh Kerala science congress, Palakkad January, p.97–9.

Uchida T, Kosugi K, Mizuyama T (2001) Effects of pipeflow on hydrological process and its relation to landslide: a review of pipeflow studies in forested headwater catchments. Hydrol Process 15:2151–2174

Weidner L., Oommen, T., Escobar-Wolf R.V., Sajinkumar K.S., Rinu S. (2018) Regional scale back-analysis using TRIGRS: An approach to advance landslide hazard modeling and prediction in sparse data regions. Landslides DOI 10.1007/s10346-018-1044-7.

Wikipedia contributors, "List of dams and reservoirs in Kerala," *Wikipedia, The Free Encyclopedia*, https://en.wikipedia.org/w/index.php?title=List_of_dams_and_reservoirs_in_Kerala&oldid=860568874 (accessed September 22, 2018).

Appendix A: Supplementary Information on Landslides

Figure A-1: Landslide that blocked the road @ 9.8263274^{O} N 76.9197930^{O} E

Figure A-2: Landslide that blocked the road @ 9.8263274^{O} N 76.9197930^{O} E

Figure A-3: Landslide near a gas station @ 9.8549653^{O} N 76.9619187^{O} E

Figure A-4: Landslide near a gas station @ 9.8549653^{O} N 76.9619187^{O} E

Figure A-5: Landslide scarp @ 9.7968694^{O} N 77.0675658^{O} E

Figure A-6: House destroyed in the landslide @ 9.7968694^{O} N 77.0675658^{O} E

Figure A-7: Interior of a house destroyed in landslide and debris flow @ 9.7966953^{O} N 77.0678775^{O} E

Figure A-8: Driveway to the house destroyed in landslide @ 9.7962622^{O} N 77.0681814^{O} E

Figure A-9: Landslide scarp @ 9.7966110^{O} N 77.0685257^{O} E

Figure A-10: Landslide scarp @ 9.7970015^{O} N 77.0683650^{O} E

Figure A-11: Large landslide in front of the newly built house @ 9.7925061^{O} N 77.0680952^{O} E

Figure A-12: Head of the landslide @ 9.7925131^{O} N 77.0680889^{O} E

Figure A-13: Minor landslide @ 9.7694732^{O} N 77.0890198^{O} E

Figure A-14: Major landslide that buried a two storey building that was in construction @ 9.7644641^{O} N 77.1096940^{O} E

Figure A-15: Debris flow failure @ 10.0830840^{O} N 77.0711627^{O} E

Figure A-16: Munnar college landslide showing piping channels @ 10.0822483^{O} N 77.0734512^{O} E

Figure A-17: Munnar college landslide showing the destroyed college building @ 10.0822577^{O} N 77.0734317^{O} E

Figure A-18: Destroyed Munnar College building @ 10.0826962^{O} N 77.0726538^{O} E

Figure A-19: Rock fall @ 10.0835676^{O} N 77.0615970^{O} E

Figure A-20: Example of soil pipping @ 10.0088136^{O} N 77.0257626^{O} E

Figure A-21: Another view of the pipping @ 10.0088132^{O} N 77.0257597^{O} E

Figure A-22: Another case showing soil pipping @ 10.0088800^{O} N 77.0258132^{O} E

Figure A-23: A landslide case with large pipping channel @ 9.9756943^{O} N 77.0216695^{O} E

Figure A-24: Another view of the pipping channel @ 9.9756741^{O} N 77.0216901^{O} E

Figure A-25: Panniyarkutty landslide that destroyed three houses and killed five people @ 9.9749966^{O} N 77.0429146^{O} E

Figure A-26: Panniyarkutty landslide @ 9.9749966^{O} N 77.0429146^{O} E

Figure A-27: Origin of the Panniyarkutty landslide @ 9.9748956^{O} N 77.0427662^{O} E

Figure A-28: Seen on the left is a house that has been destroyed in Panniyarkutty landslide @ 9.9748956^{O} N 77.0427662^{O} E

Appendix B: Supplementary Information on Flooding and Coastal and River Erosion

Figure B-1: River erosion @ 9.8575718^{O} N 76.9636035^{O} E

Figure B-2: River erosion @ 9.8575868^{O} N 76.9636007^{O} E

Figure B-3: River erosion @ 9.8585518^{O} N 76.9639427^{O} E

Appendix C: Supplementary Information on Foundation Failures

Figure C-1: Foundation of the house cracked due to ground displacement @ 9.7918757^{O} N 77.0687403^{O} E

Figure C-2: Another view of the foundation crack @ 9.7918656^{O} N 77.0687362^{O} E

Figure C-3: Another view of the foundation crack @ 9.7918219^{O} N 77.0688023^{O} E

Figure C-4: Building destroyed due to ground movement. An entire floor has been subsided @ 9.8746102^{O} N 77.1193815^{O} E

Figure C-5: Building destroyed due to ground movement. An entire floor has been subsided @ 9.8747156^{O} N 77.1193791^{O} E

Figure C-6: Column of the building destroyed due to ground movement @ 9.8746397^{O} N 77.1193175^{O} E